

RESEARCH ARTICLE

Reorganization of cerebro-cerebellar circuit in patients with left hemispheric gliomas involving language network: A combined structural and resting-state functional MRI study

Nan Zhang^{1†} | Mingrui Xia^{2,3,4†} | Tianming Qiu¹ | Xindi Wang^{2,3,4} | Ching-po Lin^{5,6,7} | Qihao Guo⁸ | Junfeng Lu¹ | Qizhu Wu⁹ | Dongxiao Zhuang¹ | Zhengda Yu¹ | Fangyuan Gong¹ | N. U. Farrukh Hameed¹ | Yong He^{2,3,4} | Jinsong Wu^{1,10} | Liangfu Zhou^{1,10}

¹Glioma Surgery Division, Department of Neurosurgery, Huashan Hospital, Fudan University, Shanghai, China

²State Key Laboratory of Cognitive Neuroscience and Learning, Beijing Normal University, Beijing, China

³Beijing Key Laboratory of Brain Imaging and Connectomics, Beijing Normal University, Beijing, China

⁴IDG/McGovern Institute for Brain Research, Beijing Normal University, Beijing, China

⁵Institute of Science and Technology for Brain-Inspired Intelligence, Fudan University, Shanghai, China

⁶Institute of Neuroscience, National Yang-Ming University, Taipei, Taiwan

⁷Brain Research Center, National Yang-Ming University, Taipei, Taiwan

⁸Department of Neurology, Huashan Hospital, Fudan University, Shanghai, China

⁹Sinorad Medical Electronics Co., Ltd, Shenzhen, China

¹⁰Shanghai Key Laboratory of Medical Image Computing and Computer Assisted Intervention, Shanghai, China

Correspondence

Jinsong Wu,

Glioma Surgery Division, Neurosurgery
Department of Huashan Hospital,
Shanghai Medical College, Fudan University,
Shanghai 200040, China.

Email: wjsongc@126.com

and

Yong He,

State Key Laboratory of Cognitive
Neuroscience and Learning,
Beijing Normal University, Beijing, 100875,
China.

Email: yong.he@bnu.edu.cn

Funding information

Beijing Municipal Science & Technology
Commission, Grant/Award Number:
Z161100000216152, Z161100000216125,
Z151100003915082; Changjiang Scholar
Professorship Award, Grant/Award Number:
T2015027; Fundamental Research Funds for
the Central Universities, Grant/Award
Number: 2017XTCX04 and 2015KJCA13;

Abstract

The role of cerebellum and cerebro-cerebellar system in neural plasticity induced by cerebral gliomas involving language network has long been ignored. Moreover, whether or not the process of reorganization is different in glioma patients with different growth kinetics remains largely unknown. To address this issue, we utilized preoperative structural and resting-state functional MRI data of 78 patients with left cerebral gliomas involving language network areas, including 46 patients with low-grade glioma (LGG, WHO grade II), 32 with high-grade glioma (HGG, WHO grade III/IV), and 44 healthy controls. Spontaneous brain activity, resting-state functional connectivity and gray matter volume alterations of the cerebellum were examined. We found that both LGG and HGG patients exhibited bidirectional alteration of brain activity in language-related cerebellar areas. Brain activity in areas with increased alteration was significantly correlated with the language and MMSE scores. Structurally, LGG patients exhibited greater gray matter volume in regions with increased brain activity, suggesting a structure–function coupled alteration in cerebellum. Furthermore, we observed that cerebellar regions with decreased brain activity exhibited increased functional connectivity with contralesional cerebro-cerebellar system in LGG patients. Together, our findings provide empirical evidence for a vital role of cerebellum and cerebro-cerebellar circuit in neural plasticity following lesional damage to cerebral

[†]Nan Zhang and Mingrui Xia contributed equally to this study.

Abbreviations: ABC, Aphasia Battery of Chinese; ACC, anterior cingulate cortex; ALFF, amplitude of low-frequency fluctuation; AQ, aphasia quotient; ASD, autism spectrum disorder; BNT, Boston Naming Test; CCD, cerebro-cerebellar diaschisis; GMV, gray matter volume; HGG, high-grade glioma; KPS, Karnofsky Performance Scale; LGG, low-grade glioma; MMSE, mini mental state examination; PCC, posterior cingulate cortex; RSFC, resting state functional connectivity; SUIT, spatially unbiased infratentorial template; VBM, voxel-based morphometry

National High Technology R&D Program of China, Grant/Award Number: 2015AAI020507; National Key Technology R&D Program of China, Grant/Award Number: 2014BAI04B05; Shanghai Municipal Commission of Health and Family Planning, Grant/Award Number: 2017YQ014; National Natural Science Foundation of China, Grant/Award Number: 81401395, 81401546, 81401479, 81401136 and 8167176

language network. Moreover, we highlight the possible different reorganizational mechanisms of brain functional connectivity underlying different levels of behavioral impairments in LGG and HGG patients.

KEYWORDS

cerebellum, glioma, language, plasticity, resting-state fMRI, structural MRI

1 | INTRODUCTION

It has long been a fundamental issue in clinical neuro-oncology to explore the pattern of functional and structural reorganization of the brain following tumor growth (Duffau, 2014; Herbet, Maheu, Costi, Lafargue, & Duffau, 2016; Kinno, Ohta, Muragaki, Maruyama, & Sakai, 2014). Such kind of research holds vital clinical significance in either facilitating the understanding of disease-specific mechanisms in the development and prognosis of diseases, or providing new insight into therapeutic targets for novel and more effective treatment interventions.

Gliomas are the most common primary brain tumors and usually cause impairments in multiple cognitive functions. However, the neural mechanisms underlying cognitive impairments in glioma patients are largely unclear (Derks et al., 2017; Derks, Reijneveld, & Douw, 2014). Convergent evidences have demonstrated that the functional and structural organization of the brain follows a communicating and dynamic network pattern, which is different from the traditional view of conceiving the brain in a localizationist and inflexible framework (Bassett & Bullmore, 2009; Duffau, 2014). In this network-based framework, brain function is precisely organized via between-node interaction in the distributed large-scale neural network, which underpins the neural substrates of behavioral and cortical reorganization after brain damage (Derks et al., 2017; Duffau, 2014; Schmähmann, 2016). Among the diverse neural functions, language function especially attracts clinical neuroscientists' attention due to its fundamental role in maintaining normal social activities on one hand, and its susceptibility to brain damage on the other hand. However, limitations of existent studies have to be addressed: first, the studies focusing on language network reorganization that underpin behavioral changes are still relatively scarce (Fang et al., 2015; Han et al., 2013; Kinno, Ohta, Muragaki, Maruyama, & Sakai, 2014; Kristo, Raemaekers, Rutten, de Gelder, & Ramsey, 2015); Tyler, Wright, Randall, Marslen-Wilson, & Stamatakis, 2010, especially in glioma patients; second, majority of current investigations regarding reorganization of language network in lesioned brains focus on cerebral cortex, and little attention has been paid to the cerebellar role in this process, which is inappropriate.

In contrast to the limited number of investigations addressing the role of cerebro-cerebellar circuit in language network reorganization following supratentorial lesion (Lidzba, Wilke, Staudt, Krageloh-Mann, & Grodd, 2008), similar studies have been extensively performed in the investigation of various higher-order cognitive functions in healthy subjects, and patients with neurodegenerative,

neurodevelopmental, neurological, and psychiatric diseases (Buckner, 2013; Buckner, Krienen, Castellanos, Diaz, & Yeo, 2011; Dirks et al., 2016; Guo et al., 2016; Kim et al., 2014; Marien et al., 2014, 2009; O'Callaghan et al., 2016; Schmähmann and Sherman, 1998). In healthy subjects, task-fMRI research on the functional topography of human cerebellum revealed that the activation areas for language were mainly located in lobule VI and Crus I with a prominently right-lateralizing pattern, which reflected crossed organizational arrangement of cerebro-cerebellar circuit (Stoodley and Schmähmann, 2009; Stoodley, Valera, & Schmähmann, 2012). Diffusion imaging analysis also confirmed the cerebellar role in reading (Travis, Leitner, Feldman, & Ben-Shachar, 2015). In pathological conditions, the role of cerebellum or cerebro-cerebellar circuit has also been extensively studied. For example, in language-impaired adolescents with autism spectrum disorder (ASD), resting state functional connectivity (RSFC) analysis revealed that these patients exhibited reduced RSFC between right Crus I and left supratentorial regulatory language areas, including superior/middle frontal gyrus, parietal areas, and anterior cingulate gyrus (D'Mello and Stoodley, 2015; Verly et al., 2014). Furthermore, the alterations of regional intrinsic neural activity, blood perfusion and white matter diffusion metrics in cerebellum after cerebral glioma resection have been illustrated (Boyer et al., 2016; Patay et al., 2014), indicating high necessity to further elucidate the reorganizational pattern of cerebro-cerebellar functional network and its relationship with neural plasticity in glioma patients.

Notably, the kinetics of gliomas are different for slow-growing (generally in years) low-grade glioma (LGG) and rapid-progressing (generally in months) high-grade glioma (HGG), which could have influence on the behavioral and underlying neural differences between the two kinds of patients. A recent behavioral study suggested that LGG patients (i.e., WHO grade II) usually exhibit intact or slightly impaired performance in extensive neurocognitive assessments, whereas HGG patients (i.e., WHO grade III/IV) usually exhibit evident cognitive impairments (Noll, Sullaway, Ziu, Weinberg, & Wefel, 2015). Furthermore, several studies comparing the plasticity induced by progressive LGG and acute stroke lesion, demonstrated that the recruitment of brain areas remote from lesions were much more efficient in slow-growing than acute lesions (Desmurget, Bonnetblanc, & Duffau, 2007; Duffau, 2014; Kong, Gibb, & Tate, 2016). However, although it has been revealed in some studies that LGG and HGG patients have different plastic mechanisms of the structures and functions in brain network (Harris et al., 2014; Van Dellen et al., 2012; Zhang et al., 2016), the different plastic

mechanisms in cerebellum and cerebro-cerebellar circuit between LGG and HGG patients are still unclear.

Motivated by the research advancements as mentioned above, we attempt to utilize resting state fMRI (rs-fMRI) and structural MRI analyses to explore the reorganization of cerebro-cerebellar system in patients with left-hemispheric gliomas involving language network. Resting state fMRI provides an unprecedented opportunity for the exploration of abnormal intrinsic functional brain architecture of various brain disorders. This is because rs-fMRI does not only overcome the inconvenience of task-fMRI in terms of patients' cooperation, but is also easier and cheaper to implement than PET and SPECT in clinical practice (Greicius, 2008; Liu et al., 2015). Thus, rs-fMRI is suitable for exploring the neural plastic mechanisms in glioma patients. To our knowledge, no research until now has investigated the plastic pattern of language network in a large group of high-homogeneity left hemispheric glioma patients from the perspective of cerebro-cerebellar circuit. We hypothesize that the growth of left-lateralized cerebral glioma involving language network areas will not only result in reorganization of both regional cerebellar neural activity and gray matter volume (GMV), but also induce alteration in cerebro-cerebellar functional network. We also hypothesize that these patterns of reorganization are different in LGG and HGG with different growth kinetics. To validate the hypotheses, we sought to employ a data-driven voxel-by-voxel approach with the following steps. First, due to the feasibility and reliability of using amplitude of low-frequency fluctuation (ALFF) as an indicator to delineate regional spontaneous brain activity (Boyer et al., 2016; Gallea et al., 2016; Li et al., 2016; Wang et al., 2011; Zang et al., 2007), we will thus localize the cerebellar regions with altered ALFF to identify the alteration of intrinsic neural activity in cerebellum. Second, a voxel-based morphometry (VBM) analysis of the cerebellum will be performed to find the correlation between structural and functional alteration. Third, the identified cerebellar regions with altered ALFF will be taken as seeds in the subsequent whole-brain RSFC analysis to explore the altered pattern of cerebro-cerebellar circuit. Finally, the correlation analysis between the linguistic/cognitive scores and the neuroimaging metrics will be performed to highlight the clinical significance of this research. Notably, we will further conduct these analyses in LGG and HGG patients, separately, to assess their possible different reorganizational mechanisms.

2 | MATERIALS AND METHODS

2.1 | Participants

We screened and collected preoperative clinical and imaging data of 260 patients who were admitted in the Glioma Surgery Division of Huashan Hospital's Neurosurgery Department from March, 2011 to November, 2016. These patients were all with left cerebral gliomas. About 85 of the 260 patients met the following criteria: (1) Pathologically confirmed glioma (based on 2007 WHO classification system) in left cerebral hemisphere (Louis et al., 2007); (2) Location of the glioma overlapped or was within language network areas proposed by Fedorenko, Hsieh, Nieto-Castanon, Whitfield-Gabrieli, and Kanwisher (2010); (3) 18–75 years old; (4) Right-handedness confirmed by

Edinburgh Handedness Inventory; (5) No symptoms of motor impairment, which was indicated by a score of grade V in the Medical Research Council (MRC) Scale for Muscle Strength (Paternostro-Sluga et al., 2008); (6) Chinese Han nationality; (7) No history of brain operation; (8) Years of education were more than nine; (9) No midline shift in the structural images, confirmed by the in situ location of midline structures (corpus callosum, septa pellucidum, third ventricle, hypothalamus, pineal region) of the brain; (10) Both structural and functional images covered the whole brain, especially the whole cerebellum; (11) Cooperated well in the linguistic/cognitive evaluation; (12) No history of other major neurological or psychiatric disorders; and (13) No alcohol or drug abuse. Seven patients were further excluded due to superfluous head movement (exceeding 3 mm in translation or 3° in rotation) during MRI scanning. Finally, the remaining 78 patients were recruited in this study.

The basic clinical information of the recruited patients was as follows: age, 39.73 ± 12.58 years; gender, 45 males and 33 females; years of education, 12.36 ± 2.96 ; tumor volume, 46.71 ± 28.64 cm³; WHO grade: 46 cases were grade II; 17 were Grade III; and 15 were Grade IV. To assess the convergence and divergence in abnormality of brain structures and functions between LGG and HGG patients, we further divided the patients into two groups according to their WHO grade. The clinical information of the 46 LGG patients and 32 HGG patients was as follows. LGG patients: age, 37.59 ± 9.50 years; gender, 26 males and 20 females; years of education, 12.00 ± 2.74 ; tumor volume, 45.92 ± 30.01 cm³. HGG patients: age, 42.81 ± 15.67 years; gender, 19 males and 13 females; years of education, 12.30 ± 2.82 ; tumor volume, 47.85 ± 26.97 cm³.

All patients underwent detailed assessment of language function by using Boston Naming Test (BNT) and Aphasia Battery for Chinese-speakers (ABC). BNT (range, 0–30) is one of the most widely used standardized aphasia measures in clinical practice, particularly for naming ability (Vogel, Maruff, & Morgan, 2010). ABC is the Chinese standardized adaptation of the Western Aphasia Battery (Lu et al., 2013; Wu et al., 2015), which includes spontaneous speech (range, 0–20), comprehension (range, 0–230), repetition (range, 0–100), and naming (range, 0–100) scores. The Aphasia Quotient (AQ) score (range, 0–100) can be calculated from these items to reflect the global severity and type of aphasia. Individuals with an AQ score less than 93.8 were considered as aphasic subjects (Kim & Na, 2004; Lu et al., 2013; Wu et al., 2015; Yang et al., 2016). In addition to the evaluation of language function, all patients underwent comprehensive assessments of performance status, motor, and general cognitive function, by using Karnofsky Performance Scale (KPS) (Karnofsky, Abelmann, & Craver, 1948), Medical Research Council (MRC) Scale for Muscle Strength, and Mini Mental State Examination (MMSE), respectively. We also recruited 47 right-handed healthy controls (HCs) by advertisement. The recruitment criteria of HCs were the same as that of patient subjects. Three HCs were excluded due to superfluous head movement during the MRI scanning. These HCs underwent the same linguistic/cognitive assessment as the glioma patients. The detailed clinical, performance status, and linguistic/cognitive information of patients and HCs is listed in Table 1, and the specific information of LGG and HGG patients is listed in Table 2.

TABLE 1 Demographic information and clinical data (all patients and HC)

	All patients (N = 78)	HC (N = 44)	T value (χ^2)	p value
Age	39.73 ± 12.58	34.57 ± 13.11	2.119 ^a	.037 ^a
Gender (male/female)	45/33	23/21	0.335 ^b	.563 ^b
Education (years)	12.36 ± 2.96	12.98 ± 3.51	-1.036 ^a	.302 ^a
Tumor volume (cm ³)	46.71 ± 28.64	NA	NA	NA
WHO grade (II/III/IV)	46/17/15	NA	NA	NA
KPS	100 (80–100)	100 (100)	-6.148 ^a	<.001 ^a
MMSE	27 (12–30)	30 (25–30)	-4.819 ^a	<.001 ^a
BNT	20.69 ± 5.17	27.93 ± 2.50	-8.715 ^a	<.001 ^a
AQ	92.82 ± 7.45	98.93 ± 1.69	-5.352 ^a	<.001 ^a
Naming	90.86 ± 9.69	97.36 ± 3.05	-4.323 ^a	<.001 ^a
Repetition	94.88 ± 8.86	99.79 ± 0.59	-3.655 ^a	<.001 ^a
Comprehension	215.71 ± 21.04	227.25 ± 4.50	-3.587 ^a	<.001 ^a
Spontaneous speech	18.46 ± 1.88	19.84 ± 0.57	-4.745 ^a	<.001 ^a

Data are presented as the mean ± SD; KPS and MMSE scores are presented as median value and range. NA, not available; WHO, World Health Organization; KPS, Karnofsky performance scale; MMSE, mini-mental state examination; BNT, Boston Naming Test; AQ, Aphasia Quotient.

^a p-value obtained using a two-sample t-test.

^b p-value obtained using Pearson's chi-square test.

All processes strictly followed the requirements of the Declaration of Helsinki. This study was approved and supervised by the Ethics Committee of Huashan Hospital. The written informed consents were obtained from the HCs and legal guardians of the patients.

2.2 | MRI data acquisition

All images of patients and HCs were obtained using a Siemens Magnetom Verio 3.0 T MRI scanner (Siemens Medical Solutions, Erlangen, Germany).

The rs-fMRI images were acquired using the following parameters: repetition time (TR) = 2,000 ms; echo time (TE) = 35 ms; flip angle = 90°; field of view = 240 × 240 mm²; matrix size = 64 × 64; thickness/gap = 4 mm/1 mm; voxel size = 3.3 × 3.3 × 5.0 mm³; slice number = 33; scanning time = 8 min; and number of time points = 240.

All subjects were required to remain still with their eyes closed and not fall asleep. In order to stabilize the magnets, each run was preceded with 6-s dummy scans (Qiu et al., 2014).

The structural images of HCs were acquired using an axial magnetization-prepared rapid gradient echo (MPRAGE) T1-weighted sequence with high resolution, and the following parameters: TR = 1,900 ms; TE = 2.93 ms; flip angle = 90°; FOV = 250 × 219 mm; matrix size = 256 × 215; slice thickness = 1 mm; voxel size = 1 × 1 × 1 mm³; slice number = 176; and scanning time = 7 min 47 s. For gliomas with enhancement, structural images were acquired using the previous T1 weighted sequence with contrasts (gadopentetate dimeglumine). For gliomas without enhancement, except for the MPRAGE T1-weighted sequence, structural images were also acquired using an axial T2-weighted fluid-attenuated inversion recovery (T2-flair)

TABLE 2 Demographic information and clinical data (LGG/HGG patients and HC)

	HGG (N = 32)	LGG (N = 46)	HC (N = 44)	F value (χ^2)	p value	Post hoc
Age	42.81 ± 15.67	37.59 ± 9.50	34.57 ± 13.11	3.950	.022 ^a	HGG > HC
Gender (male/female)	19/13	26/20	23/21	0.397	.820 ^b	NA
Education (years)	12.30 ± 2.82	12.00 ± 2.74	12.98 ± 3.51	1.262	.287 ^a	NA
Tumor volume (cm ³)	47.85 ± 26.97	45.92 ± 30.01	NA	NA	.771	NA
WHO grade	Grade III: 17; Grade IV: 15	Grade II: 46	NA	NA	NA	NA
KPS	90 (80–100)	100 (90–100)	100 (100)	21.084	<.001 ^a	HGG < HC; LGG < HC
MMSE	27 (12–30)	28 (14–30)	30 (25–30)	15.223	<.001 ^a	HGG < LGG < HC
BNT	19.09 ± 6.08	21.80 ± 4.14	27.93 ± 2.50	43.809	<.001 ^a	HGG < LGG < HC
AQ	90.29 ± 9.38	94.58 ± 5.17	98.93 ± 1.69	20.508	<.001 ^a	HGG < LGG < HC
Naming	86.52 ± 11.98	93.88 ± 6.27	97.36 ± 3.05	19.896	<.001 ^a	HGG < LGG < HC
Repetition	92.63 ± 10.57	96.46 ± 7.16	99.79 ± 0.59	9.829	<.001 ^a	HGG < HC; LGG < HC
Comprehension	207.59 ± 27.36	221.35 ± 12.76	227.25 ± 4.50	13.866	<.001 ^a	HGG < LGG < HC
Spontaneous speech	18.21 ± 2.27	18.63 ± 1.55	19.84 ± 0.57	11.965	<.001 ^a	HGG < HC; LGG < HC

Data are presented as the mean ± SD; KPS and MMSE scores are presented as median value and range. NA, not available; WHO, World Health Organization; KPS, Karnofsky performance scale; MMSE, mini-mental state examination; BNT, Boston Naming Test; AQ, Aphasia Quotient.

^a p-value obtained using ANOVA.

^b p-value obtained using Pearson's chi-square test.

^c p-value obtained using independent two-sample t test between HGG and LGG.

sequence with the following parameters: TR = 9,000 ms; TE = 99 ms; flip angle = 150°; FOV = 240 × 214 mm; matrix size = 256 × 160; slice thickness = 2 mm; voxel size = 0.9 × 1.3 × 2.0 mm³; slice number = 66; and scanning time = 7 min 30 s.

2.3 | Imaging data preprocessing

2.3.1 | Tumor overlapping image construction

This procedure was achieved manually using RANO criteria as reference (Wen et al., 2010). A neurosurgeon (ZN) used MRICron (<http://people.cas.sc.edu/rorden/mcron.html>) to trace tumors on individual 3D structural images: T1 enhancement images for gliomas with enhancement, and T2-flair images coregistered to T1 weighted images for gliomas without enhancement. A senior neurosurgeon (WJS) confirmed the accuracy of the manual tracing. After manually tracing the tumor, we created a tumor mask for each patient. After spatial normalization to standard MNI space, all patients' tumor masks were stacked together and binarized to construct a tumor overlapping image (Figure 1), in which each voxel was identified as tumor regions, at least for one patient. This tumor image was further overlapped with a whole brain gray matter (GM) mask (obtained by thresholding the GM probability map in SPM12 with probability larger than 0.2) to

obtain the final patients' group mask, which restricted further RSFC analysis to nontumor GM regions. The lesion overlapping result, and the relationship between glioma location and language network template for all patients, LGG patients and HGG patients are shown in Figure 1.

2.3.2 | rs-fMRI data preprocessing

This procedure was performed using Statistical Parametric Mapping 12 (SPM 12; Wellcome Department of Imaging Neuroscience, University College London, UK) and the toolkit of Data Processing and Analysis for Brain Imaging (DPABI) (Yan, Wang, Zuo, & Zang, 2016). The rs-fMRI data was preprocessed as follows. We first excluded the first 10 time points in order to eliminate the potential influence of subjects' adaptation to the scanning environment at the beginning of imaging data collection. Following this, slice timing and realignment were performed to correct temporal differences and head motion, respectively. The criterion for head motion was set as 3 mm in translation and 3° in rotation. Seven patients and three HCs were excluded for exceeding this criterion, leaving the data of 78 patients and 44 HCs for further analysis. Following these procedures, spatial normalization was performed according to the transformation field obtained when

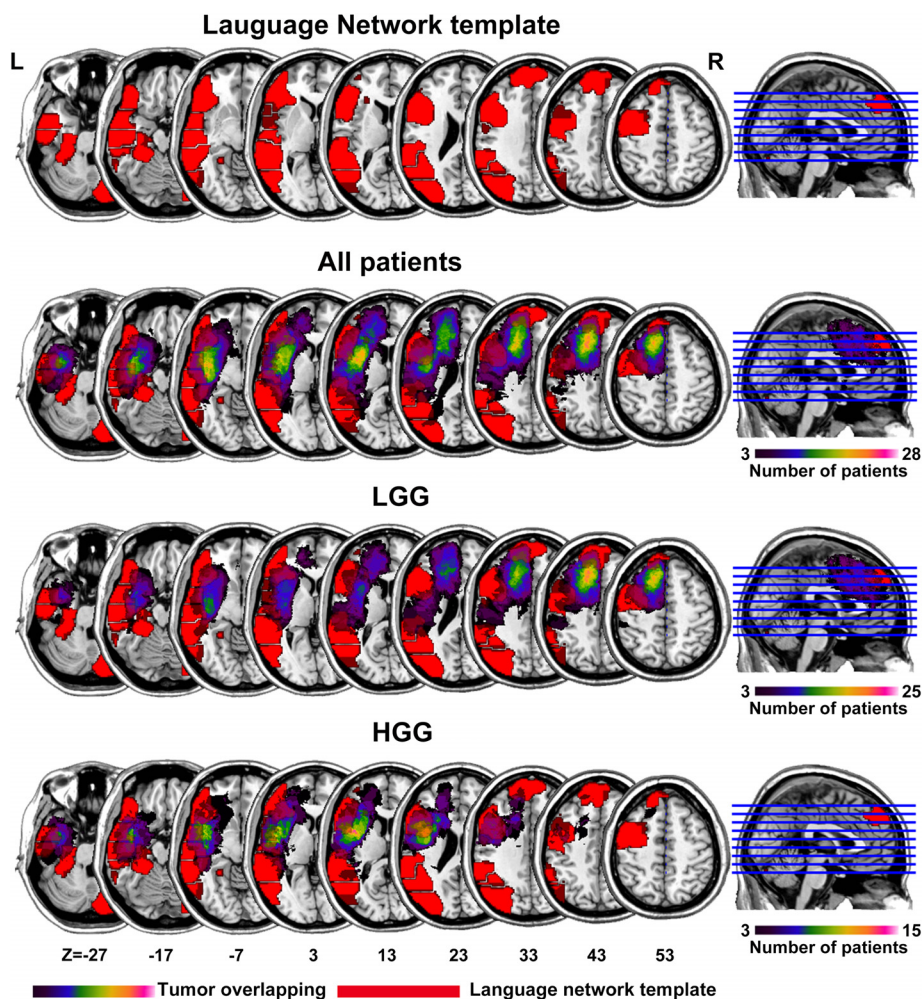


FIGURE 1 Tumor topography and overlap between tumor and language network template. The areas overlapped by the tumors of all patients, LGG patients and HGG patients are separately presented on the brain. The color bar represents the number of patients with a lesion on a specific voxel. The red color indicates brain areas overlapped by the language network template [Color figure can be viewed at wileyonlinelibrary.com]

individual T1 images were projected to Montreal Neurological Institute (MNI) space. In the spatial normalization procedure, we first coregistered native T1 images to rs-fMRI images and segmented T1 images. Then, 12-parameter affine transformation and nonlinear deformation were used to normalize the segmented T1 images to MNI space. Particularly, we used cost function masking (CFM) method with the tumor area masked to improve the precision of spatial normalization in glioma patients (Andersen, Rapcsak, & Beeson, 2010; Brett, Leff, Rorden, & Ashburner, 2001). The transformation parameters obtained from structural images were subsequently applied to normalize the functional images to MNI space. The functional images were further resampled to an isolated resolution of $3 \times 3 \times 3 \text{ mm}^3$ and were smoothed using a Gaussian kernel with full-width at the half maximum (FWHM) of 4 mm. The linear trend was removed for the time series of each voxel, and several nuisance signals were regressed out, including the Friston's 24 head motion parameter (Friston, Williams, Howard, Frackowiak, & Turner, 1996), white matter and cerebrospinal fluid signals (Yan, Cheung, et al., 2013a). Notably, we did not regress out global signal here because this procedure remains controversial. Finally, a temporal band-pass filtering (0.01–0.08 Hz) was applied to the time courses.

2.4 | Cerebellar spontaneous neural activity analysis

To examine the regional spontaneous brain activity in the cerebellum, we calculated the ALFF (Zang et al., 2007; Zhang et al., 2010) for the time series of each voxel within the cerebellum. Previous studies have suggested that low-frequency BOLD signals are related to neuronal electrophysiological activity and local field potential (Logothetis, Pauls, Augath, Trinath, & Oeltermann, 2001; Shmuel & Leopold, 2008), and that ALFF quantifying the amplitude of low frequency oscillations of the BOLD signal is supposed to partly reflect the amplitude of the spontaneous neuronal electrophysiological activity (Zhang et al., 2010). This method has been widely used to investigate the activities of abnormal regional brain activities in a broad range of neuropsychiatric disorders (Boyer et al., 2016; Gallea et al., 2016; Li et al., 2016; Van Hees et al., 2014; Wang et al., 2011; Yang et al., 2016; Zhang et al., 2010). Briefly, the power spectral density was obtained by transforming each voxel's time series to frequency domain. As the power of a given frequency proportioned with the square of the amplitude of this frequency, the square root of the power spectrum at each frequency can be calculated, and the subsequent averaged square root across 0.01–0.08 Hz at each voxel was considered as the ALFF of this voxel. We then standardized each individual ALFF map by subtracting the average value and divided by the standard deviation of the ALFF value of the cerebellum (Yan, Craddock, et al., 2013b; Yang et al., 2016). The calculation of ALFF and further statistical analysis were restricted within cerebellum by using the spatially unbiased infratentorial template (SUIT) mask, which is a high-resolution template of human cerebellum (D'Mello, Crocetti, Mostofsky, & Stoodley, 2015). This template was generated by applying automatic cerebellum segmentation and nonlinear normalization algorithms based on T1-weighted structural MRI data, and its reliability was validated on independent dataset (Diedrichsen, 2006).

2.5 | Cerebellar gray matter volume analysis

To explore the structural basis of the altered cerebellar neural activity, we used VBM method to estimate cerebellar GMV of each participant. The processing of structural images included the following procedures by using SPM12: (1) Segmenting the T1 structural images into gray matter, white matter and cerebrospinal fluid; (2) Putting all the glioma patients' and HCs' T1 images together, importing the segmentation parameter files into Diffeomorphic Anatomical Registration Through Exponentiated Lie Algebra (DARTEL) (Ashburner, 2007), and creating a specific template for this study; (3) Projecting the segmented tissues into MNI space by affine transformation; and (4) Smoothing the obtained images by using a Gaussian kernel with FWHM of 4 mm. We finally used the normalized, modulated, and smoothed data for statistical analysis within the SUIT mask.

2.6 | Cerebro-cerebellar resting-state functional connectivity analysis

In order to study the reorganization of cerebro-cerebellar RSFC in glioma patients, we performed the following seed-based functional connectivity analysis. The seeds were selected as the regions showing significant group difference in ALFF (Gallea et al., 2016; Li et al. 2014, 2016; Van Hees et al., 2014). For each seed, we then extracted averaged time course of the seed region, and calculated Pearson correlation coefficients between the seed's time course and all the other voxels'. Fisher's *r*-to-*z* transformation was further performed on the coefficients map to improve normality. Notably, the RSFC analysis was constrained within the patients' group mask, which excluded tumor regions.

2.7 | Statistical analysis

The comparisons of age, years of education, performance status, and linguistic/cognitive scores between all patients and HCs were achieved by independent two-sample *t*-tests. The comparison of gender composition was achieved by Pearson Chi-square test. To further elucidate the differences in the demographic information and behavioral scores among LGG patients, HGG patients, and HCs, one-way analysis of variance (ANOVA) was performed with independent two-sample *t*-tests as post hoc pairwise comparisons analyses. The above-mentioned statistics were performed using SPSS 21.0.

We employed nonparametric permutation tests to compare the voxel-wise cerebellar ALFF, GMV, and cerebro-cerebellar RSFC between patients and HCs (Eklund, Nichols, & Knutsson, 2016; Nichols & Holmes, 2002; Winkler, Ridgway, Webster, Smith, & Nichols, 2014). This procedure was accomplished using Statistical nonParametric Mapping (SnPM) toolbox (<http://www.nitrc.org/projects/snpm/>) for SPM12. Briefly, by applying general linear model (GLM), SnPM constructs pseudo *t*-statistic images to assess for significance using a standard nonparametric multiple comparisons procedure based on permutation testing. The permutation times was set at a default of 5,000. As suggested in a recent study that nonparametric permutation test is able to precisely control false positive rate in the cluster-level inference (Eklund et al., 2016), we set the significance level as the cluster-forming threshold of 0.01 with family-wise error

(FWE) corrected cluster $p < .05$. The statistical analyses of ALFF and GMV were performed within the SUIT-mask and that of FC was conducted in the patients' group mask. Similarly, to assess the alteration of these brain imaging metrics in LGG and HGG patients' groups, the nonparametric permutation tests were also performed between each pair of the LGG, HGG, and HC groups. Notably, age, gender, and years of education were treated as covariates in all between-group statistical analyses.

To assess the clinical significance of the identified abnormal structural and functional regions in glioma patients, we extracted the mean values (ALFF, GMV, or RSFC) in regions showing significant between-group difference, and used Pearson's partial correlation analysis to investigate their relationship to clinical or cognitive scores. Similar to the previously reported analytic method of imaging-behavioral correlation in patients with lesions (Griffis et al., 2017; Lunven et al., 2015), we treated years of education, glioma WHO grade, and glioma volume as covariates in the correlation analyses. The statistical significance level was set as $p < .05$, uncorrected.

2.8 | Validation analysis

To evaluate the reliability and reproducibility of our main results, we additionally adopted procedures for reducing head motion artifact by performing 'scrubbing' method on the preprocessed images and re-analyzed the obtained data (Power, Barnes, Snyder, Schlaggar, & Petersen, 2012; Yan, Cheung, et al., 2013a). In the scrubbing procedure, we censored rs-fMRI volumes that were with sudden head motion, based on the criterion of framewise displacement (FD) above 0.5 mm. One volume before and two volumes after the bad volume were discarded during the censoring. The calculations of ALFF and FC were then re-analyzed using the censored data.

Considering that the latest 2016 WHO classification system of glioma (Louis et al., 2016) incorporates molecular markers while simultaneously maintaining the grading system similar to that of 2007 WHO classification system (i.e., the molecular characteristics would not alter the diagnosis of tumor grade), we regrouped the glioma patients according to their molecular pathological information to exclude the subtype of LGGs that are with potential malignant biological behavior similar to that of HGG. Specifically, LGG patients with IDH wild type (IDH-wt), different from the LGG patients with IDH mutation (IDH-mutant), are usually with similar poor prognosis to that of HGG (Louis et al., 2016). We thus analyzed the tumor samples of all the 78 glioma patients to obtain the molecular pathological information by using genetic sequencing method (50 cases) and immunohistochemical method (28 cases). And we found that in the 46 LGG patients, 7 were IDH-wt and the other 39 were IDH-mutant. After that, we cautiously re-performed statistical analysis of cerebellar ALFF and GMV by excluding the 7 IDH-wt LGG patients (i.e., comparison of the two metrics between all 71 glioma patients and 44 HCs, and pairwise between-group comparison of the two metrics among 39 IDH-mutant LGG patients, 32 HGG patients and 44 HCs). In this procedure, age, gender, and years of education were also treated as covariates to be regressed out.

3 | RESULTS

3.1 | Demographic, performance status, and linguistic/cognitive information of subjects

There was no significant difference in gender (Chi square test, $\chi^2 = 0.335$, $p = .563$) or educational level (two sample t -test, $t [120] = -1.036$, $p = .302$) between the left hemispheric glioma patients and HCs. The patient group had significantly higher age than the control groups (two sample t -test, $t [120] = 2.144$, $p = .037$). Regarding behavior scores, the glioma patients had significantly lower KPS, MMSE, BNT and all of the 5 ABC scores than HCs (two-sample t -test, all p values $< .001$, Table 1).

The comparison among LGG patients, HGG patients, and HCs revealed that there were no group effects in gender (Chi square test, $\chi^2 = 0.335$, $p = .820$) or years of education (ANOVA, $F [2,119] = 1.262$, $p = .287$). Significant group effect was observed in age among three groups (ANOVA, $F [2,119] = 3.950$, $p = .022$), which was mainly resulted from the higher age in the HGG group as compared with the HC group. Besides, both LGG and HGG patients had significantly lower KPS, MMSE, BNT, AQ, naming, repetition, comprehension, and spontaneous speech scores than HCs (ANOVA, $p < .001$). Moreover, as compared with LGG patients, HGG patients exhibited significantly lower scores in MMSE, BNT, AQ, naming and comprehension (two-sample t -test, all p values $< .001$, Table 2).

3.2 | Abnormal cerebellar ALFF in glioma patients

In the comparison between all patients and HCs, the left hemispheric glioma patients exhibited decreased ALFF in the lateral part of right lobule VIIa and increased ALFF in the medial part of left lobule VIIa (permutation test, FWE corrected $p < .05$) (Figure 2a and Table 3).

Further pairwise comparisons among LGG, HGG, and HC groups revealed that both LGG and HGG patients had decreased ALFF in the lateral part of right lobule VIIa and increased ALFF in the medial part of left lobule VIIa as compared with HCs (permutation test, FWE corrected $p < .05$), indicating a similar cerebellar abnormal pattern of ALFF in the two patient groups. Additionally, LGG patients showed marginally significant decreased ALFF in vermis III/IV/V (permutation test, uncorrected $p = .0047$, FWE corrected $p = .0508$) (Figure 2a and Table 3). No significant differences were found between LGG and HGG patients.

3.3 | Correlation between ALFF and linguistic/cognitive and performance status variables

In all patients, Pearson's partial correlation analysis revealed that ALFF in left cerebellar lobule VIIa was positively correlated with BNT score ($r = .272$, $p = .018$), AQ score ($r = .230$, $p = .047$), naming score ($r = .267$, $p = .021$), and comprehension score ($r = .306$, $p = .008$) significantly (Figure 2b). No significant correlation was observed between KPS score and ALFF.

Comparably, in HGG patients, significantly positive correlations were observed between regional ALFF in the left cerebellar lobule VIIa and linguistic/cognitive scores, including the BNT score ($r = .479$,

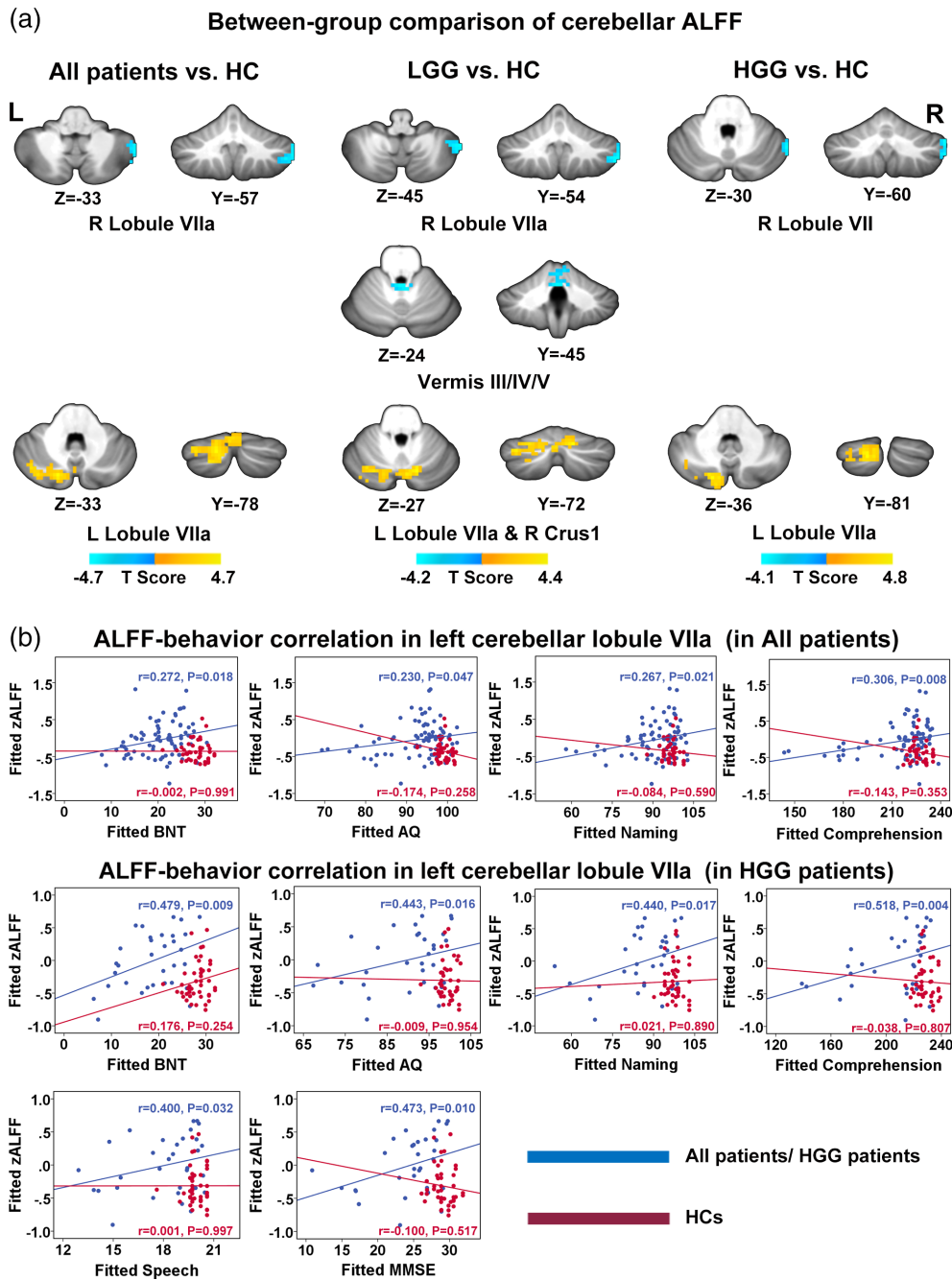


FIGURE 2 Altered cerebellar ALFF and its relationship with behavioral score in patients. (a) Between-group (all patients vs. HC, LGG vs. HC and HGG vs. HC) differences in ALFF within the cerebellum. Hot and cold colors in the color bar indicate increased and decreased ALFF, respectively, in the patient group (permutation test, FWE corrected $p < .05$). (b) the scatter plot map displays the significant partial correlation results between increased ALFF (all patients > HC and HGG > HC) and cognitive/linguistic scores. The partial correlation results were obtained after treating education level, glioma WHO grade and tumor volume as covariates. Fitted ALFF and fitted linguistic/cognitive scores indicate the sum of the mean value and the residual value of ALFF and linguistic/cognitive scores after regressing out education level, glioma WHO grade, and tumor volume. In HC group, the WHO grade and tumor volume was set as zero when performing partial correlation analysis. ALFF, amplitude of low-frequency fluctuation; BNT, Boston naming test; AQ, aphasia quotient [Color figure can be viewed at wileyonlinelibrary.com]

$p = .009$), AQ score ($r = .443$, $p = .016$), naming score ($r = .440$, $p = .017$), comprehension score ($r = .518$, $p = .004$), spontaneous speech score ($r = .400$, $p = .032$), and MMSE score ($r = .473$, $p = .010$) (Figure 2b). There was no significant correlation between KPS score and regional ALFF in HGG patients.

No significant correlation between cerebellar regions with altered ALFF and linguistic/cognitive and performance status scores was observed in LGG group and HC group (Figure 2b).

3.4 | Altered cerebellar gray matter volume in glioma patients

As compared with HCs, left hemispheric glioma patients had larger GMV in the medial part of bilateral cerebellar lobule VIIa (permutation test, FWE corrected $p < .05$) (Figure 3a and Table 4). The region showing increased GMV (all patients > HC, the region in the left panel of Figure 3a) highly overlapped with the region exhibiting increased

TABLE 3 Regions with significant between-group difference in cerebellar ALFF

Cluster	Region	Size (mm ³)	Peak MNI coordinate	Patient vs. HC	T value	Corrected cluster <i>p</i> value
All patients vs. HC						
1	Right lobule VIIa	1998	(54,-57,-33)	Patients<HC	-4.6343	.0222
2	Left lobule VIIa	6,426	(-15,-78,-33)	Patients>HC	4.6979	.0002
LGG vs. HC						
1	Right lobule VIIa	1,431	(54,-54,-45)	LGG < HC	-3.7892	.0310
2	Vermis III/IV/V	1,188	(0,-45,-24)	LGG < HC	-4.1291	.0508 (.0047) ^a
3	Left lobule VIIa Right lobule Crus1	5,373	(15,-72,-27)	LGG > HC	4.3633	.0002
HGG vs. HC						
1	Right lobule VII	1917	(54,-60,-30)	HGG < HC	-4.1297	.0040
2	Left lobule VIIa	4,455	(-15,-81,-36)	HGG > HC	4.8542	.0004

Significance level was set as $p < .01$ at voxel level with FWE corrected $p < .05$ at cluster level, permutation test.

^a Uncorrected cluster *p*-value.

ALFF (all patients > HC, the region in the second row of the left panel of Figure 2a). The overlapping volume was 1,701 mm³, which was obtained by calculating the volume of the overlapping region in the MNI space. Moreover, in the overlapped region, the mean ALFF value positively correlated with the mean GMV value in the patient group ($r = .347$, $p = .002$) (Figure 3b), suggesting a structural–functional coupled cerebellar alteration in glioma patients.

In the comparison between LGG patients and HCs, we observed that LGG patients had larger GMV in the medial part of bilateral cerebellar lobule VIIa than HCs (permutation test, FWE corrected $p < .05$) (Figure 3a and Table 4). The overlapping volume between regions with increased GMV (LGG > HC, the region in the right panel of Figure 3a) and increased ALFF (LGG > HC, the region in the third row of the middle panel of Figure 2a) reached 1,674 mm³. Similarly, we found a significantly positive correlation between the mean ALFF value and the mean GMV in this overlapping region in LGG patients ($r = .393$, $p = .007$) (Figure 3b).

No significant differences in cerebellar GMV were found between HGG patients and HCs or between LGG and HGG patients.

Furthermore, no significant correlation between cerebellar regions with altered GMV and linguistic/cognitive and performance status scores was observed in the all patient group, LGG patient group, and HC group.

3.5 | Abnormal cerebro-cerebellar RSFC in glioma patients

For each between-group comparison (i.e., all patients vs. HC, LGG vs. HC, and HGG vs. HC), the regions showing between-group differences in ALFF were chosen as seeds for RSFC analyses. Here, given that vermis III/IV/V exhibited a marginally significant between-group difference (FWE corrected $p = .0508$) and its potential importance in language processing (Lesage, Nailor, & Miall, 2016; Yang, Wu, Weng, & Bandettini, 2014), we also included this area as seed region in RSFC analysis.

We did not find any significant differences in cerebro-cerebellar RSFC between all patients and HCs, or between HGG patients and

HCs. However, in the comparison between LGG patients and HCs, the cerebellar vermis III/IV/V exhibited significantly higher RSFC to right thalamus, anterior cingulate cortex (ACC), and posterior cingulate cortex (PCC) in LGG patients as compared with HCs (permutation test, FWE corrected $p < .05$) (Figure 4 and Table 5). Additionally, using a lenient significance threshold (permutation test, voxel level $p < .01$, uncorrected cluster level $p < .01$), LGG patients exhibited increased RSFC between lateral part of right lobule VIIa and left cerebellar lobule VII/VIII, right medial prefrontal cortex, right angular gyrus (rAG), right inferior parietal lobule (rIPL) and right middle, and superior frontal gyri (rMFG/SFG) (Supporting Information Figure S1 and Supporting Information Table S1). LGG patients also showed increased RSFC of the cerebellar vermis III/IV/V with left cerebellar lobule VII/VIII and rMFG/SFG (Supporting Information Figure S2 and Supporting Information Table S2).

3.6 | Correlation between RSFC and linguistic/cognitive and performance status variables

In LGG patients, Pearson's partial correlation analysis revealed that mean FC value in right thalamus, PCC and ACC was significantly positively correlated with comprehension score ($r = .348$, $p = .018$, uncorrected) (Figure 4c). No significant correlation was observed between FC and KPS, MMSE, AQ, naming, repetition, and spontaneous speech scores.

In HC group, no significant correlations between mean FC value in right thalamus, PCC and ACC, and linguistic/cognitive or performance status scores were found.

3.7 | Validation results

We estimated the effect of head motion by conducting scrubbing procedure on the pre-processed images. No subjects were excluded according to a criterion of less than 5 min of data remaining after censoring (Dai et al., 2015). Re-analyses of the scrubbed images demonstrated basically consistent results with the main results (Supporting Information Figures S3 and S4; Supporting Information Table S3). However, for RSFC analysis of the vermis III/IV/V in the comparison

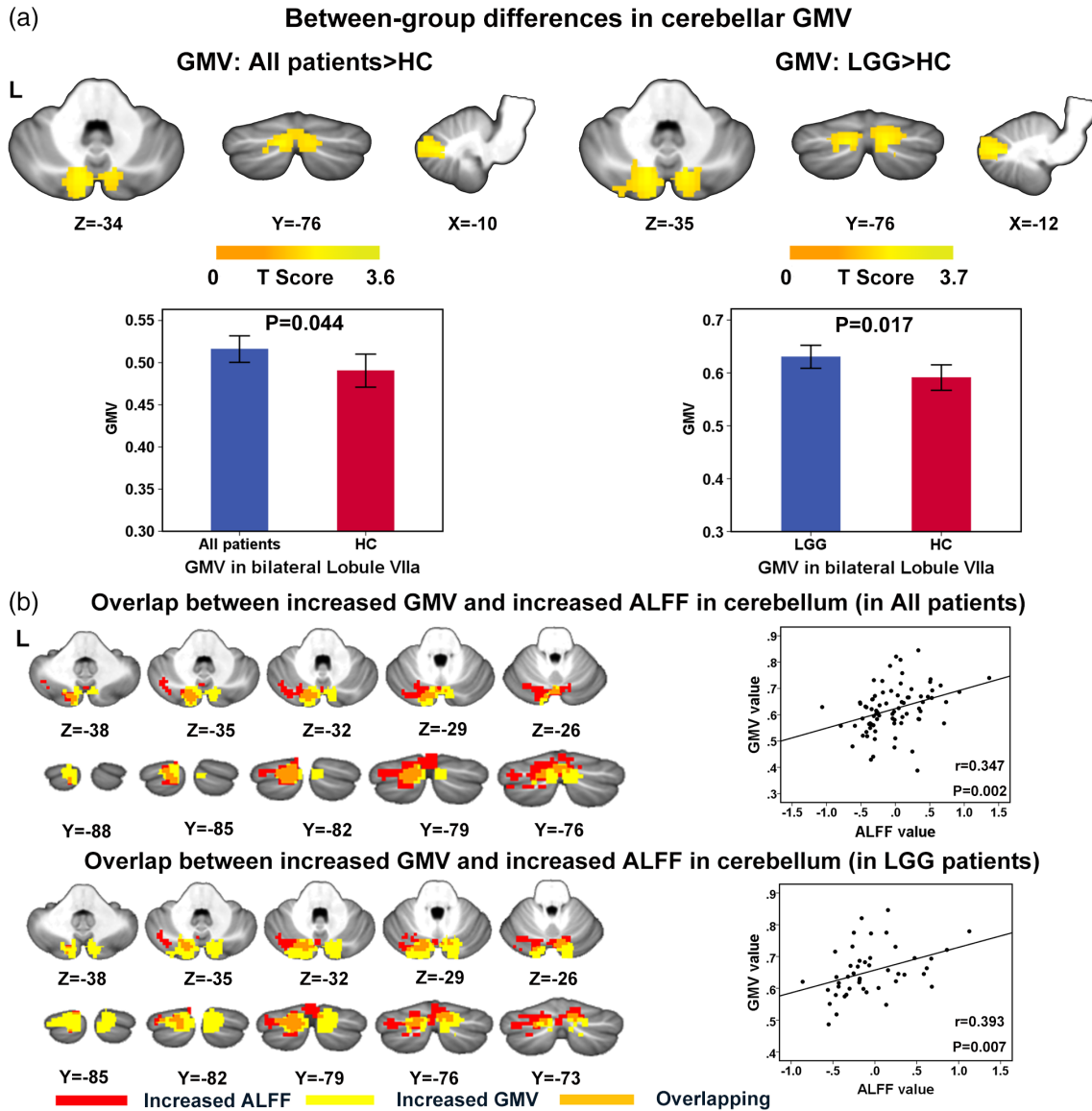


FIGURE 3 Between-group differences in cerebellar GMV and overlap between increased GMV and increased ALFF. (a) Between-group comparison showed that the GMV in the bilateral lobule VIIa is greater in all patients as compared with HCs (left), and also in LGG patients compared with HCs (right). Color-bars denote the T value (permutation test, $p < .01$ in voxel level and <0.05 in cluster level, FWE corrected). The lower row demonstrates the comparison of GMV (mean value) within the cluster in which between-group differences in GMV were observed. The error bars represent standard deviations. (b) Overlap map between regions with increased GMV and increased ALFF, the maps of all patients and LGG patients are shown separately. The scatter plots in the right column of each row demonstrate the correlation between mean ALFF value and mean GMV value in the overlapping region. GMV, gray matter volume; ALFF, amplitude of low-frequency fluctuation [Color figure can be viewed at wileyonlinelibrary.com]

between LGG patients and HCs, the increased RSFC in LGG patients was mainly located in right thalamus and PCC (Supporting Information Figure S5 and Supporting Information Table S4).

After excluding the 7 IDH-wt LGG patients, we re-performed statistical analysis of cerebellar ALFF and GMV. Finally, the reanalysis indicated that when considering the molecular subtypes (especially the condition of

TABLE 4 Regions with significant between-group difference in gray matter volume

Cluster	Region	Size (mm ³)	Peak MNI coordinate	Patient vs. HC	T value	Corrected cluster p value
All patients vs. HC						
1	Left lobule VIIa Right lobule VIIa	4,688	(-10,-76,-34)	Patients>HC	3.5487	.0434
LGG vs. HC						
1	Right lobule VIIa	4,208	(12,-74,-34)	LGG > HC	3.6104	.0500
2	Left lobule VIIa	4,264	(-12,-76,-34)	LGG > HC	3.7154	.0490

Significance level was set as $p < .01$ at voxel level with FWE corrected $p < .05$ at cluster level, permutation test.

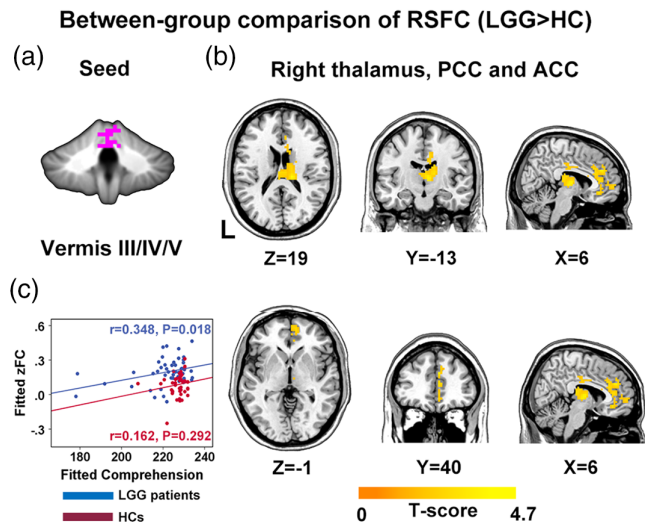


FIGURE 4 Between-group differences in cerebro-cerebellar RSFC. The LGG group exhibited significantly higher cerebro-cerebellar RSFC (b) than HC group for seed vermis III/IV/V (a) (permutation test, $p < .01$ in voxel level and $p < .05$ in cluster level, FWE corrected). Color-bars indicate the T value. The mean RSFC value in right thalamus, ACC and PCC region was positively correlated with comprehension score in LGG patients (c). RSFC, resting-state functional connectivity; PCC, posterior cingulate cortex; ACC, anterior cingulate cortex [Color figure can be viewed at wileyonlinelibrary.com]

IDH mutation) of LGG, the alteration of cerebellar ALFF and GMV in glioma patients were basically consistent with the main results, which proved the robustness of the main findings of this article (Supporting Information Figures S8 and S9; Supporting Information Tables S5 and S6).

4 | DISCUSSION

In this study, we adopted a pure data-driven approach to investigate the glioma-induced abnormalities of structural and functional alterations in cerebellum from regional viewpoint, and reorganization of cerebro-cerebellar functional connectivity from integrative viewpoint. This research yielded the following principal findings: (i) Both LGG and HGG patients with left cerebral hemispheric glioma involving language network exhibited alterations in cerebellar neural activity when compared with HCs, characterized by a decrease of ALFF in right cerebellar lobule VIIa and an increase of ALFF in left cerebellar lobule VIIa. LGG patients also exhibited decreased ALFF in vermis III/IV/V. Positive correlations between neural activity and linguistic/cognitive evaluation scores in all patients and HGG patients were also corroborated; (ii) The alteration of increased cerebellar neural activity shared similar spatial pattern with that of increased GMV, whereas

decreased cerebellar neural activity was independent of structural change. Notably, when comparing LGG and HGG patients separately with HCs, such a pattern was only observed in LGG patients; (iii) Compared with HCs, LGG patients exhibited increased RSFC between cerebellar areas with decreased neural activity and the areas subserving higher-order language-related cognitive functions in right cerebral hemisphere and right thalamus. Such a pattern was nonexistent in HGG patients. Furthermore, the increased RSFC in LGG patients was positively correlated with linguistic scores.

To our knowledge, this is the first investigation focusing on the reorganization of cerebro-cerebellar network in patients with cerebral glioma involving language network by employing structural and functional neuroimaging analyses methods from both regional and integrative perspectives.

4.1 | Functional and structural alteration of the cerebellum

As revealed in this research, the changes in cerebellar intrinsic functional activity subsequent to left cerebral hemispheric glioma follow a bidirectional pattern. The interpretation of such results should go along two parallel lines:

- (i) Mechanism of neural reorganization in lesioned brain. The evident functional and structural alteration in cerebellum revealed in our research strongly suggests the significant role of cerebellum in the plasticity of patients with supratentorial lesions. The phenomenon of decreased intrinsic neural activity in contralesional cerebellum can be interpreted with crossed cerebro-cerebellar-diaschisis (CCD) mechanism (Carrera & Tononi, 2014), which suggests decreased blood perfusion in contralesional cerebellar hemisphere following damage to the supratentorial areas (Patay et al., 2014), thus causing decrease in intrinsic neural activity in the corresponding cerebellar areas (Boyer et al., 2016). We notice that no significant correlations between decreased ALFF and linguistic/cognitive scores were observed, such result indicates the possibility that the decrease of neural activity in the contralesional cerebellar hemisphere might be an inherent response to cerebral damage (CCD mechanism). There might be correlation between decreased cerebellar ALFF and linguistic/cognitive scores at the beginning stage of left cerebral gliomas. However, considering the ethical factor, it is difficult to capture the dynamic progress of glioma to determine the relationship between cerebellar ALFF and behavioral scores, because the malignant nature of glioma requires resection as early as possible once diagnosis is established. Thus, the precise imaging-behavior correlation between decreased cerebellar ALFF and linguistic/cognitive functions in patients with cerebral damage can be indirectly determined via

TABLE 5 Regions with significant between-group difference in RSFC (LGG vs. HC)

Seed	Region	Size (mm ³)	Peak MNI coordinate	Mean strength		T value	Corrected cluster p value
				LGG	HC		
Vermis III/IV/V	Right thalamus ACC/PCC	13,338	(15,-24,18)	0.20 ± 0.12	0.08 ± 0.10	4.6250	.0392

Significance level was set as $p < .01$ at voxel level with FWE corrected $p < .05$ at cluster level, permutation test.

longitudinal research in glioma patients with intact behavioral and imaging data in preoperative and different post-operative time points. Conversely, the increased intrinsic neural activity in ipsilesional cerebellar lobule VIIa can be interpreted as the result of compensation for the disruption of the cerebro-cerebellar circuit with lesion, as indicated by the positive correlation between the increased ALFF and linguistic/cognitive scores.

- (ii) The role of cerebellum in brain network subserving language and cognitive function. Numerous studies in healthy people and clinical cases have verified that the topography of linguistic function within the cerebellum is lateralized to the right lobule VI/VIIa and midline lobule VII/VIII (Marien et al., 2014; Marvel & Desmond, 2010; Petersen, Fox, Posner, Mintun, & Raichle, 1988; Stoodley & Schmahmann, 2009). In our research, the altered cerebellar neural activity was mainly located in bilateral lobule VIIa. This result is consistent with, but not confined to, the view that the effect of anatomical damage extends to areas distant from the location of the lesion, but remains within the bounds of the network in which the lesion existed (Baldassarre, Ramsey, Siegel, Shulman, & Corbetta, 2016; Nomura et al., 2010). Furthermore, our finding can be taken as a supplement to the mechanism of functional reorganization following tumor invasion (Desmurget et al., 2007), in that the recruitment of ipsilesional and contralesional hemisphere should extend to the framework of cerebro-cerebellar circuit. Additionally, LGG patients exhibited decreased ALFF in vermal lobule III/IV/V, which was traditionally considered to subserve motor-related function (Stoodley and Schmahmann, 2009). Given that all recruited patients in this research were free of motor impairment, this result might imply the potential role of the cerebellar region in the motor-element of language. Such result was comparable to the finding that supratentorial "nontypical" (e.g., motor-related area) language areas participated in language reorganization following cerebral damage (Desmurget et al., 2007; Thiel et al., 2001). Our results can be further supported from a previous PET study in which patients with left cerebral tumor had decreased activation in right cerebellar lobule VI/VII and increased activation in left cerebellar lobule VI/VII during the verb generation task (Thiel et al., 2001).

Our research also demonstrated the structural alteration of cerebellum following supratentorial glioma (especially LGG) growth. We found similar pattern between increased cerebellar neural activity and increased cerebellar GMV, whereas decreased cerebellar neural activity was independent of structural change. This finding is similar to the matched pattern of ALFF and GMV alteration in patients with orthostatic tremor (Gallea et al., 2016). Our result hints that the alteration of cerebellar intrinsic neural activity was closely related to, but not totally dependent on, structural alteration, and such phenomenon is especially evident in LGG patients. Besides, our research indicates a selective vulnerability of cerebellar structure and function following the intrinsic connectivity network pattern in focally damaged patients similar to that unraveled in neurodegenerative diseases (Guo et al., 2016; Schmahmann, 2016), solidifying the idea that the cerebellum should be viewed as an active participator in the process of lesion-induced neural plasticity.

4.2 | Alteration of cerebro-cerebellar functional connectivity

Patients with supratentorial LGG invading language network also exhibited altered pattern in cerebro-cerebellar RSFC, presented with elevated RSFC between cerebellar areas with decreased ALFF and areas belonging to the contralesional cerebro-cerebellar circuit, including right thalamus, rSFG, rMFG, rAG, rIPL, left cerebellar lobule VII, and ACC/PCC (Figure 4; Supporting Information Figures S1 and S2). However, it should reinforce the point that such alteration in cerebro-cerebellar RSFC only exists in LGG, rather than HGG patients. Such finding demonstrates the potentially indispensable position of the cerebro-cerebellar circuit in the plastic process following injury to cerebral language network. The cerebro-cerebellar circuit, in which the thalamus relays information between contralateral cerebellum and ipsilateral cerebral cortex, is precisely organized in a crossed pattern (Buckner, 2013; De Smet, Paquier, Verhoeven, & Marien, 2013; Habas et al., 2009). Therefore, it is easy to understand the elevated RSFC between right thalamus and cerebellar regions with decreased ALFF. Here, it should be noted that including the vermis III/IV/V as a seed in RSFC analysis was according to a relatively lenient statistical threshold (FWE corrected $p = .0508$). Thus, the results of this seed should be taken as an explorative finding, which remains to be validated in future studies. Nevertheless, the alteration pattern of cerebro-cerebellar RSFC in glioma patients was physiologically meaningful, or at least indicative of the trend of glioma-induced alteration in cerebro-cerebellar RSFC.

Notably, the interpretation of increased cerebro-cerebellar RSFC is uncertain. Here, we propose two alternative ways of interpretation. The first interpretation is to view the increased RSFC as the recruitment and establishment of new circuits to compensate for the disrupted ipsilesional counterpart. The positive correlation between FC value in right thalamus, and ACC/PCC and the comprehension score further supported this speculation. The recruitment of homologous language-related areas in the contralesional cerebral hemisphere has been extensively verified in stroke and glioma patients (Desmurget et al., 2007; Duffau 2014; Thiel et al., 2005; Winhuisen et al., 2005; Yang et al., 2016). Moreover, areas with increased RSFC have been corroborated to participate in the complex procedure of language processing. For example, SFG and MFG in the dominant hemisphere are charged with higher-order cognitive control, whereas dominant AG and IPL primarily undertake the role of linguistic comprehension (Fedorenko & Thompson-Schill, 2014; Wu et al., 2015). Furthermore, dominant MFG has been robustly verified to play a special role in Chinese language processing (Hu et al., 2010; Siok, Niu, Jin, Perfetti, & Tan, 2008; Tan, Xu, Chang, & Siok, 2013; Wu et al., 2015). The second interpretation is to view the increased RSFC between network regions (i.e., hyperconnectivity) as a fundamental response to neurological disruption in patients with focal lesions or neurodegenerative/psychiatric diseases (Derks et al., 2014; Hillary & Grafman, 2017; Hillary et al., 2015). When a primary communication pathway is disrupted by focal lesion, to maintain efficient information processing, the less-established routes based on detour pathways will be more involved in information transmission, resulting in the increase of connections, clustering, and path length to relevant brain hubs, thus benefiting the

injured network while simultaneously balancing metabolic cost and communication efficiency (Hillary & Grafman, 2017; Derks et al., 2017; Liang, Zou, He, & Yang, 2013). In our research, the regions with increased cerebro-cerebellar RSFC, including thalamus, SFG, MFG, AG, IPL and ACC/PCC, have been defined as brain hubs in literature (Buckner et al., 2009; Tomasi & Volkow, 2010; Van den Heuvel, Kahn, Goni, & Sporns, 2012). In this sense, the cerebro-cerebellar hyperconnectivity in LGG patients might be a presentation of the common phenomenon in this particular group of patients, rather than the presentation of compensation. In summary, regardless of which viewpoint reflects the exact reorganizational mechanism, our finding strengthens the importance of cerebro-cerebellar circuit in terms of lesion-induced language or cognitive plasticity.

4.3 | The influence of glioma on connectivity of default mode network

Another important finding is the increased RSFC between cerebellar areas with decreased ALFF and the cerebral cortex conceived as belonging to default mode network (DMN)—rAG, PCC, and ACC (Greicius, Srivastava, Reiss, & Menon, 2004). We assume this result might be due to the disruption of network interactions between behavior-specific network (language network in this research) and DMN following brain injury. Our finding is similar to the disruption of anti-correlation between dorsal attention network (DAN) and DMN in stroke patients with attention deficit (Baldassarre et al., 2016; Ramsey et al., 2016). Such an assumption could be elucidated in the future by investigating the longitudinal changes in the interaction between language network and DMN before and after tumor resection.

Notably, although the number is very limited and the conclusions are inconsistent, some articles have reported the change of DMN connectivity in glioma patients (Derks et al., 2017; Esposito et al., 2012; Ghumman, Fortin, Noel-Lamy, Cunnane, & Whittingstall, 2016; Harris et al., 2014; Van Dellen et al., 2012; Zhang et al., 2016). Esposito et al. first specifically reported the modifications of DMN connectivity in 24 patients with left cerebral gliomas. They found global reduction of DMN connectivity and a more right-lateralized DMN in LGG patients than HGG patients and HCs (Esposito et al., 2012). Ghumman et al. also identified reduced DMN connectivity in patients with brain tumors in different localizations, and they particularly found left cerebral gliomas to exert the largest influence on DMN connectivity, regardless of tumor size, and type, whereas such an effect was absent in right hemispheric tumors (Ghumman et al., 2016). In contrast, the results in another research indicated that the location and WHO grade of glioma correlated with the impairment of DMN integrity, which was different from the findings in the previous study (Harris et al., 2014). Moreover, Derks et al. performed an in-depth analysis of the spatial properties of the network disturbances caused by glioma, and analyzed the relationship between whole-brain functional connectomic profiles and clinical characteristics. They defined hubs as regions belonging to DMN and frontoparietal network (FPN), and they observed that glioma patients particularly exhibited increased connectivity between hubs and nonhubs. Additionally, the increased hub-nonhub connectivity, and the connectivity distributions were more evident in LGG patients than in HGG patients. The altered functional

connectomic profiles were also related to performance status and progression-free survival (Derks et al., 2017). Although the adopted analytic methods in our research were different from those in Derks' study, the results, that cerebellar regions with altered ALFF showed increased FC with areas of ACC/PCC and rAG in LGG patients, were very similar. Considering the large sample size in both Derks' and our research, we hold the viewpoint that increased DMN connectivity, rather than decreased DMN connectivity, should be the prevalent alteration following glioma growth.

4.4 | LGG and HGG: Behavioral and neural reorganizational differences

Our research also demonstrates the behavioral and neural reorganizational differences in LGG and HGG patients.

Behaviorally, both LGG and HGG patients had lower language/cognitive scores than HCs, whereas HGG patients performed worse than LGG patients did. Such results are highly consistent with previous studies investigating the correlation between neurocognitive function and glioma grade, in that LGG patients were frequently associated with normal or slightly impaired neurocognitive functions, while HGG patients usually suffered from more evident neurocognitive impairment (Desmurget et al., 2007; Noll et al., 2015; Taphoorn & Klein, 2004). Moreover, our results provide further insight into the differences in cognitive capacities (especially, linguistic abilities) between LGG/HGG patients and HCs, which is different from previous studies that merely focused on comparisons of neurocognitive functions among patients harboring different grades of gliomas (Noll et al., 2015; Taphoorn & Klein, 2004).

Mechanically, LGG and HGG patients exhibited almost identical patterns of alteration in spontaneous brain activity in cerebellum when compared with HCs, and no differences in cerebellar functional activity were observed between LGG and HGG patients. These results indicate that cerebral LGG and HGG have a similar effect on cerebellar neural activity. We also demonstrated a positive correlation between ALFF in the medial part of left lobule VIIa and language function in all patients (particularly in HGG patients) (Figure 2b), while such imaging-behavioral correlation was absent in LGG patients. Furthermore, LGG patients, rather than HGG patients, exhibited structural-functional coupled alteration in cerebellum and RSFC alteration in cerebro-cerebellar system, when compared with HCs. These results might imply the different plastic mechanisms that follow gliomas with varying growth kinetics. Specifically, the absence of correlation between increased cerebellar ALFF and linguistic/cognitive scores in LGG patients might be due to a gradual recruitment of contralesional cerebro-cerebellar circuit to maintain normal or slightly-impaired linguistic/cognitive functions in LGG patients, for the speculation that the slowly progressive nature of LGG allows such process in a slow and gradual manner, as indicated by coupled functional-structural alteration in cerebellum. Similarly, the fact that the increased cerebro-cerebellar RSFC was only observed in LGG patients, rather than in HGG patients, might also result from the different growth kinetics of gliomas, since the slow-growing nature of LGG causes more evident hyperconnectivity than HGG does (Derks et al., 2017; Van Dellen et al., 2012). Conversely, the significant correlation between increased

cerebellar ALFF and linguistic/cognitive scores in HGG patients might come from a relatively rapid recruitment of the cerebellar part of contralesional cerebro-cerebellar circuit in order to offset the rapid impairment of linguistic/cognitive functions caused by rapid growth of glioma. The absence of functional-structural coupling in cerebellum and cerebro-cerebellar RSFC alteration in HGG patients might also be due to the fast-growing nature of HGG not allowing enough time to cause such effect. Together, the observed different patterns of reorganization in LGG and HGG patients provide first-hand evidence for the neural mechanism underlying the differential plasticity following acute and slow-growing brain lesions (Desmurget et al., 2007; Duffau 2014).

4.5 | Language and cognitive clinical significance

The positive correlation between ALFF in the medial part of left lobule VIIa and language function in all patients (particularly in HGG patients) (Figure 2b) suggests that this cerebellar zone is involved in language processing. We believe these identified imaging-behavioral correlations to be language-related according to the following reasons. First, recruitment of patients in this study was rigorously controlled, only those right-handed patients with left hemispheric glioma invading language network areas were enrolled (Figure 1) (Fedorenko et al., 2010). Second, considering the glioma's possible influence on motor-related cerebro-cerebellar circuit, all recruited patients were confirmed to be motor-intact, thus ensuring that the identified alterations in cerebellum and cerebro-cerebellar circuit were not related to motor deficit. Third, we observed significant correlations between brain activities and linguistic evaluation scores, rather than KPS scores which represented performance status. Finally, the identified cerebro-cerebellar areas with structural and functional alterations were traditionally viewed with high language-relevancy according to previous knowledge (as discussed above) (Marien et al., 2014; Stoodley 2012; Stoodley & Schmahmann, 2009; Stoodley & Stein, 2011; Verly et al., 2014). These facts, therefore, suggest the language-related significance of this study.

However, we have to realize that the findings revealed in this study could not be absolutely concluded as language-specific. First, positive correlation was also observed between increased cerebellar ALFF and MMSE (indication of general cognition) in HGG patients (Figure 2b). Second, the subjects in this study only underwent MMSE (general cognition) and ABC (language function) evaluation, the comprehensive assessments of other multiple cognitive domains were unavailable, there thus exists possible correlation between imaging alteration and other cognitive functions. Third, the fact that MMSE scale contains language element has to be taken into account. Specifically, we found significantly positive correlations between the language scores and the MMSE score in patients (e.g., $r = .792$, $p < .001$ between AQ and MMSE; $r = .766$, $p < .001$ between Comprehension and MMSE; Supporting Information Figure S7). Furthermore, we treated AQ, which was a comprehensive indicator of language functional status, as an additional covariate to recalculate the relationship between cerebellar increased ALFF and MMSE score in HGG patients. After regressing out the effect of AQ, the partial correlation analysis revealed nonsignificant correlation between cerebellar increased ALFF

and MMSE score in HGG patients ($r = .209$, $p = .285$), suggesting that the relationship between ALFF and MMSE could be partly explained by the variance of patients' language ability. Finally, the phenomenon of hyperconnectivity in glioma patients might be a fundamental alteration in pathological condition. Thus, more extensive evaluation of language and multidomain cognitive functions and further analysis of imaging-behavior correlation in the future will elucidate this problem.

From the perspective of translational application in clinical practice, the observed structural and functional alterations in cerebellum and cerebro-cerebellar circuit may potentially be developed as therapeutic targets for linguistic or cognitive rehabilitation using transcranial magnetic stimulation (TMS) or transcranial direct cortical stimulation (tDCS), as that has been investigated in healthy people or patients with psychiatric/psychological disorders (D'Mello, Turkeltaub, & Stoodley, 2017; Gallea et al., 2016; Grimaldi et al., 2016; Halko, Farzan, Eldaief, Schmahmann, & Pascual-Leone, 2014; Pope & Miall, 2012). Additionally, we have identified the cerebellar regions that are related with language/cognitive function, reminding us to pay attention to the preservation of linguistic/cognitive function when performing surgery on cerebellum. This issue may be clarified via investigating the dynamic changes of language and cognitive function before and after cerebellar tumor resection.

4.6 | Limitations and future directions

Several limitations of this study need to be addressed. First, the patient group had a significantly higher age than the HC group ($p = .037$). Although we specifically treated age as regressed covariate in the statistical models, group-level results might still be influenced by age effect. The correlation analyses revealed significant negative correlation between age and GMV, but no significant correlations were found between age and functional metrics (Supporting Information Figure S6). To strictly control the potential influence of age, we excluded five HCs to match the ages between all patients and HCs (all patients: 39.73 ± 12.58 vs. HCs: 36.15 ± 13.10 , $p = .155$). Following this, the between-group differences remained significant in cerebellar ALFF ($p < .001$) and GMV ($p = .025$), indicating that our primary findings were independent of age effect. However, age effect should be carefully controlled in participant recruitments. Second, we investigated general language function, rather than specific language-related sub-skills (i.e., phonemic, semantic, reading, etc.). Investigation of cerebro-cerebellar role in the mechanism underlying reorganization of specific language sub-skill is thus called on in the future. Third, as discussed in the previous part, the clinical significance of the imaging finding cannot either be totally concluded or absolutely excluded as language-specific, for the unavailability of extensive evaluation of multiple cognitive functions other than language function. More comprehensive assessments of language and multidomain cognitive functions are thus required to strengthen the language or cognitive significance of the imaging findings. Fourth, the pathological stratification in this study was based on the 2007 WHO classification system. The new 2016 WHO classification system further incorporates molecular information, which shows that molecular glioma subtype (e.g., IDH-mutant or IDH-wt) is an important factor that influences the prognosis, especially in LGG patients. Generally speaking, IDH-wt

LGGs usually cause poorer prognosis than IDH-mutant LGGs do (Louis et al., 2016). Although our team has demonstrated that not all IDH-wt LGG patients are with poor prognosis (Aibaidula et al., 2017) (in fact, the T1 and T1 contrast images also demonstrated that no obvious destructive effect that similar to HGG was observed in the IDH-wt LGG patients, see Supporting Information Figure S10), we still took measures to control the potential influence of molecular characteristics on the main findings of our research, by excluding the IDH-wt LGG patients. Following this procedure, the validation analysis demonstrated that the main findings regarding the different plastic mechanisms of cerebellar ALFF and GMV between LGG and HGG patients were robust. However, in order to make the conclusion more strict and convincing, the new 2016 WHO classification system should be adopted in the future studies. Fifth, to facilitate group comparisons of cerebro-cerebellar RSFC, we created a "group mask" which excluded all voxels overlapped by tumors (Figure 1). The BOLD signal tightly adjacent to tumor was thus naturally ignored at the individual level during this process. However, we have to bear in mind the important role of brain tissues, situated in the perilesional area and ipsilesional cerebral hemisphere, in the neural plastic process (Desmurget et al., 2007; Duffau, 2014; Kristo et al., 2015). From this viewpoint, investigating the changes in RSFC or large-scale functional networks following brain injury at the individual level is required in the future. Sixth, we did not perform therapeutic intervention to testify the clinical significance of the observed functional and structural alterations in cerebellum and cerebro-cerebellar circuit. As mentioned above, therapeutic interventions, such as TMS or tDCS on cerebellum have been applied to improve language/cognitive function or induce brain network reorganization (D'Mello et al., 2017; Gallea et al., 2016; Grimaldi et al., 2016; Halko et al., 2014; Pope & Miall, 2012). How to precisely interfere with these targets, in an evoking or inhibitive manner, is necessary to be elucidated in the future to achieve the translational significance. Finally, this research is a cross-sectional design. Future prospective longitudinal studies focusing on the dynamic changes of cerebro-cerebellar circuit and its relationship with language or cognitive function will better delineate the mechanisms of language or cognitive plasticity in glioma patients before and after surgery, thereby facilitating the identification of both imaging biomarkers for better prognostic monitoring, and modulation targets.

5 | CONCLUSION

To our knowledge, this research is the first to suggest that functional reorganization of cerebro-cerebellar circuit subserves the neural plasticity after invasion of language network by dominant cerebral hemispheric glioma. Glioma growth does not only result in reorganization of both regional neural activity and GMV in language-related area in cerebellum, but also induces alteration, or at least a trend of alteration, in cerebro-cerebellar functional network. Besides, this research also unravels the possible different plastic mechanisms underlying different levels of behavioral impairments in LGG and HGG patients. Altogether, this study expands our understanding of the mechanism of neural plasticity following lesion-induced damage to language network, and more broadly, provides a new perspective to deepen the

research on the plastic mechanisms following lesion-induced damage to cerebrum.

ACKNOWLEDGMENTS

The authors wish to thank MRI technician (Zhong Yang) and neuropsychologists (Yan Zhou) for MRI and behavioral data collection. They thank Dr. Abudumijit Aibaidula for molecular pathological information. They also appreciate Dr. Yanchao Bi, Yuxing Fang and Binke Yuan, of Beijing Normal University, China, for their advice on the analysis of data.

ORCID

Nan Zhang  <https://orcid.org/0000-0002-9960-6859>

Mingrui Xia  <https://orcid.org/0000-0003-4615-9132>

Yong He  <https://orcid.org/0000-0002-7039-2850>

Jinsong Wu  <https://orcid.org/0000-0001-7854-9798>

REFERENCES

- Aibaidula, A., Chan, A. K. Y., Shi, Z. F., Li, Y. X., Zhang, R. Q., Yang, R., ... Ng, H. K. (2017). Adult IDH wild-type lower-grade gliomas should be further stratified. *Neuro-Oncology*, *19*, 1327–1337.
- Andersen, S. M., Rapcsak, S. Z., & Beeson, P. M. (2010). Cost function masking during normalization of brains with focal lesions: Still a necessity? *NeuroImage*, *53*, 78–84.
- Ashburner, J. (2007). A fast diffeomorphic image registration algorithm. *NeuroImage*, *38*, 95–113.
- Baldassarre, A., Ramsey, L. E., Siegel, J. S., Shulman, G. L., & Corbetta, M. (2016). Brain connectivity and neurological disorders after stroke. *Current Opinion in Neurology*, *29*, 706–713.
- Bassett, D. S., & Bullmore, E. T. (2009). Human brain networks in health and disease. *Current Opinion in Neurology*, *22*, 340–347.
- Boyer, A., Deverdun, J., Duffau, H., Le Bars, E., Molino, F., de Champfleure, N. M., & Bonnetblanc, F. (2016). Longitudinal changes in cerebellar and thalamic spontaneous neuronal activity after wide-awake surgery of brain tumors: A resting-state fMRI study. *Cerebellum*, *15*, 451–465.
- Brett, M., Leff, A. P., Rorden, C., & Ashburner, J. (2001). Spatial normalization of brain images with focal lesions using cost function masking. *NeuroImage*, *14*, 486–500.
- Buckner, R. L. (2013). The cerebellum and cognitive function: 25 years of insight from anatomy and neuroimaging. *Neuron*, *80*, 807–815.
- Buckner, R. L., Krienen, F. M., Castellanos, A., Diaz, J. C., & Yeo, B. T. (2011). The organization of the human cerebellum estimated by intrinsic functional connectivity. *Journal of Neurophysiology*, *106*, 2322–2345.
- Buckner, R. L., Sepulcre, J., Talukdar, T., Krienen, F. M., Liu, H. S., Hedden, T., ... Johnson, K. A. (2009). Cortical hubs revealed by intrinsic functional connectivity: Mapping, assessment of stability, and relation to Alzheimer's disease. *Journal of Neuroscience*, *29*, 1860–1873.
- Carrera, E., & Tononi, G. (2014). Diaschisis: Past, present, future. *Brain*, *137*, 2408–2422.
- D'Mello, A. M., Crocetti, D., Mostofsky, S. H., & Stoodley, C. J. (2015). Cerebellar gray matter and lobular volumes correlate with core autism symptoms. *NeuroImage Clinical*, *7*, 631–639.
- D'Mello, A. M., & Stoodley, C. J. (2015). Cerebro-cerebellar circuits in autism spectrum disorder. *Frontiers in Neuroscience*, *9*, 408.
- D'Mello, A. M., Turkeltaub, P. E., & Stoodley, C. J. (2017). Cerebellar tDCS modulates neural circuits during semantic prediction: A combined tDCS-fMRI study. *The Journal of Neuroscience*, *37*, 1604–1613.
- Dai, Z., Yan, C., Li, K., Wang, Z., Wang, J., Cao, M., ... He, Y. (2015). Identifying and mapping connectivity patterns of brain network hubs in Alzheimer's disease. *Cerebral Cortex*, *25*, 3723–3742.

- De Smet, H. J., Paquier, P., Verhoeven, J., & Marien, P. (2013). The cerebellum: Its role in language and related cognitive and affective functions. *Brain and Language*, 127, 334–342.
- Derks, J., Dirkson, A. R., de Witt Hamer, P. C., van Geest, Q., Hulst, H. E., Barkhof, F., ... Douw, L. (2017). Connectomic profile and clinical phenotype in newly diagnosed glioma patients. *Neuroimage Clinical*, 14, 87–96.
- Derks, J., Reijneveld, J. C., & Douw, L. (2014). Neural network alterations underlie cognitive deficits in brain tumor patients. *Current Opinion in Oncology*, 26, 627–633.
- Desmurget, M., Bonnetblanc, F., & Duffau, H. (2007). Contrasting acute and slow-growing lesions: A new door to brain plasticity. *Brain*, 130, 898–914.
- Diedrichsen, J. (2006). A spatially unbiased atlas template of the human cerebellum. *NeuroImage*, 33, 127–138.
- Dirkx, M. F., den Ouden, H., Aarts, E., Timmer, M., Bloem, B. R., Toni, I., & Helmich, R. C. (2016). The cerebral network of Parkinson's tremor: An effective connectivity fMRI study. *The Journal of Neuroscience*, 36, 5362–5372.
- Duffau, H. (2014). The huge plastic potential of adult brain and the role of connectomics: New insights provided by serial mappings in glioma surgery. *Cortex*, 58, 325–337.
- Eklund, A., Nichols, T. E., & Knutsson, H. (2016). Cluster failure: Why fMRI inferences for spatial extent have inflated false-positive rates. *Proceedings of the National Academy of Sciences of the United States of America*, 113, 7900–7905.
- Esposito, R., Mattei, P. A., Briganti, C., Romani, G. L., Tartaro, A., & Caulo, M. (2012). Modifications of default-mode network connectivity in patients with cerebral glioma. *PLoS One*, 7, e40231.
- Fang, Y., Han, Z., Zhong, S., Gong, G., Song, L., Liu, F., ... Bi, Y. (2015). The semantic anatomical network: Evidence from healthy and brain-damaged patient populations. *Human Brain Mapping*, 36, 3499–3515.
- Fedorenko, E., Hsieh, P. J., Nieto-Castanon, A., Whitfield-Gabrieli, S., & Kanwisher, N. (2010). New method for fMRI investigations of language: Defining ROIs functionally in individual subjects. *Journal of Neurophysiology*, 104, 1177–1194.
- Fedorenko, E., & Thompson-Schill, S. L. (2014). Reworking the language network. *Trends in Cognitive Sciences*, 18, 120–126.
- Friston, K. J., Williams, S., Howard, R., Frackowiak, R. S., & Turner, R. (1996). Movement-related effects in fMRI time-series. *Magnetic Resonance in Medicine*, 35, 346–355.
- Gallea, C., Popa, T., Garcia-Lorenzo, D., Valabregue, R., Legrand, A. P., Apartis, E., ... Vidailhet, M. (2016). Orthostatic tremor: A cerebellar pathology? *Brain*, 139, 2182–2197.
- Ghumman, S., Fortin, D., Noel-Lamy, M., Cunnane, S. C., & Whittingstall, K. (2016). Exploratory study of the effect of brain tumors on the default mode network. *Journal of Neuro-Oncology*, 128, 437–444.
- Greicius, M. (2008). Resting-state functional connectivity in neuropsychiatric disorders. *Current Opinion in Neurology*, 21, 424–430.
- Greicius, M. D., Srivastava, G., Reiss, A. L., & Menon, V. (2004). Default-mode network activity distinguishes Alzheimer's disease from healthy aging: Evidence from functional MRI. *Proceedings of the National Academy of Sciences of the United States of America*, 101, 4637–4642.
- Griffis, J. C., Nenert, R., Allendorfer, J. B., Vannest, J., Holland, S., Dietz, A., & Szafarski, J. P. (2017). The canonical semantic network supports residual language function in chronic post-stroke aphasia. *Human Brain Mapping*, 38, 1636–1658.
- Grimaldi, G., Argyropoulos, G. P., Bastian, A., Cortes, M., Davis, N. J., Edwards, D. J., ... Celnik, P. (2016). Cerebellar transcranial direct current stimulation (ctDCS): A novel approach to understanding cerebellar function in health and disease. *The Neuroscientist*, 22, 83–97.
- Guo, C. C., Tan, R., Hodges, J. R., Hu, X., Sami, S., & Hornberger, M. (2016). Network-selective vulnerability of the human cerebellum to Alzheimer's disease and frontotemporal dementia. *Brain*, 139, 1527–1538.
- Habas, C., Kamdar, N., Nguyen, D., Prater, K., Beckmann, C. F., Menon, V., & Greicius, M. D. (2009). Distinct cerebellar contributions to intrinsic connectivity networks. *The Journal of Neuroscience*, 29, 8586–8594.
- Halko, M. A., Farzan, F., Eldaief, M. C., Schmahmann, J. D., & Pascual-Leone, A. (2014). Intermittent theta-burst stimulation of the lateral cerebellum increases functional connectivity of the default network. *The Journal of Neuroscience*, 34, 12049–12056.
- Han, Z., Ma, Y., Gong, G., He, Y., Caramazza, A., & Bi, Y. (2013). White matter structural connectivity underlying semantic processing: Evidence from brain damaged patients. *Brain*, 136, 2952–2965.
- Harris, R. J., Bookheimer, S. Y., Cloughesy, T. F., Kim, H. J., Pope, W. B., Lai, A., ... Ellingson, B. M. (2014). Altered functional connectivity of the default mode network in diffuse gliomas measured with pseudo-resting state fMRI. *Journal of Neuro-Oncology*, 116, 373–379.
- Herbet, G., Maheu, M., Costi, E., Lafargue, G., & Duffau, H. (2016). Mapping neuroplastic potential in brain-damaged patients. *Brain*, 139, 829–844.
- Hillary, F. G., & Grafman, J. H. (2017). Injured brains and adaptive networks: The benefits and costs of Hyperconnectivity. *Trends in Cognitive Sciences*, 21, 385–401.
- Hillary, F. G., Roman, C. A., Venkatesan, U., Rajtmajer, S. M., Bajo, R., & Castellanos, N. D. (2015). Hyperconnectivity is a fundamental response to neurological disruption. *Neuropsychology*, 29, 59–75.
- Hu, W., Lee, H. L., Zhang, Q., Liu, T., Geng, L. B., Seghier, M. L., ... Price, C. J. (2010). Developmental dyslexia in Chinese and English populations: Dissociating the effect of dyslexia from language differences. *Brain*, 133, 1694–1706.
- Karnofsky, D. A., Abelmann, W. H., & Craver, L. F. (1948). The use of nitrogen mustards in the palliative treatment of carcinoma. *Cancer*, 1, 634–656.
- Kim, D. J., Kent, J. S., Bolbecker, A. R., Sporns, O., Cheng, H., Newman, S. D., ... Hetrick, W. P. (2014). Disrupted modular architecture of cerebellum in schizophrenia: A graph theoretic analysis. *Schizophrenia Bulletin*, 40, 1216–1226.
- Kim, H., & Na, D. L. (2004). Normative data on the Korean version of the western aphasia battery. *Journal of Clinical and Experimental Neuropsychology*, 26, 1011–1020.
- Kinno, R., Ohta, S., Muragaki, Y., Maruyama, T., & Sakai, K. L. (2014). Differential reorganization of three syntax-related networks induced by a left frontal glioma. *Brain*, 137, 1193–1212.
- Kong, N. W., Gibb, W. R., & Tate, M. C. (2016). Neuroplasticity: Insights from patients harboring gliomas. *Neural Plasticity*, 2016, 2365063.
- Kristo, G., Raemaekers, M., Rutten, G. J., de Gelder, B., & Ramsey, N. F. (2015). Inter-hemispheric language functional reorganization in low-grade glioma patients after tumour surgery. *Cortex*, 64, 235–248.
- Lesage, E., Nailer, E. L., & Miall, R. C. (2016). Cerebellar BOLD signal during the acquisition of a new lexicon predicts its early consolidation. *Brain and Language*, 161, 33–44.
- Li, F., He, N., Li, Y., Chen, L., Huang, X., Lui, S., ... Gong, Q. (2014). Intrinsic brain abnormalities in attention deficit hyperactivity disorder: A resting-state functional MR imaging study. *Radiology*, 272, 514–523.
- Li, F., Lui, S., Yao, L., Hu, J. M., Lv, P. L., Huang, X. Q., ... Gong, Q. Y. (2016). Longitudinal changes in resting-state cerebral activity in patients with first-episode schizophrenia: A 1-year follow-up functional MR imaging study. *Radiology*, 279, 867–875.
- Liang, X., Zou, Q. H., He, Y., & Yang, Y. H. (2013). Coupling of functional connectivity and regional cerebral blood flow reveals a physiological basis for network hubs of the human brain. *Proceedings of the National Academy of Sciences of the United States of America*, 110, 1929–1934.
- Lidzba, K., Wilke, M., Staudt, M., Krageloh-Mann, I., & Grodd, W. (2008). Reorganization of the cerebro-cerebellar network of language production in patients with congenital left-hemispheric brain lesions. *Brain and Language*, 106, 204–210.
- Liu, F., Guo, W. B., Fouche, J. P., Wang, Y. F., Wang, W. Q., Ding, J. R., ... Chen, H. F. (2015). Multivariate classification of social anxiety disorder using whole brain functional connectivity. *Brain Structure & Function*, 220, 101–115.
- Logothetis, N. K., Pauls, J., Augath, M., Trinath, T., & Oeltermann, A. (2001). Neurophysiological investigation of the basis of the fMRI signal. *Nature*, 412, 150–157.
- Louis, D. N., Ohgaki, H., Wiestler, O. D., Cavenee, W. K., Burger, P. C., Jouvet, A., ... Kleihues, P. (2007). The 2007 WHO classification of tumours of the central nervous system. *Acta Neuropathologica*, 114, 97–109.

- Louis, D. N., Perry, A., Reifenger, G., von Deimling, A., Figarella-Branger, D., Cavenee, W. K., ... Ellison, D. W. (2016). The 2016 World Health Organization classification of tumors of the central nervous system: A summary. *Acta Neuropathologica*, 131, 803–820.
- Lu, J., Wu, J., Yao, C., Zhuang, D., Qiu, T., Hu, X., ... Zhou, L. (2013). Awake language mapping and 3-tesla intraoperative MRI-guided volumetric resection for gliomas in language areas. *Journal of Clinical Neuroscience*, 20, 1280–1287.
- Lunven, M., Thiebaut de Schotten, M., Bourlon, C., Duret, C., Migliaccio, R., Rode, G., & Bartolomeo, P. (2015). White matter lesional predictors of chronic visual neglect: A longitudinal study. *Brain*, 138, 746–760.
- Marien, P., Ackermann, H., Adamaszek, M., Barwood, C. H., Beaton, A., Desmond, J., ... Ziegler, W. (2014). Consensus paper: Language and the cerebellum: An ongoing enigma. *Cerebellum*, 13, 386–410.
- Marien, P., Baillieux, H., De Smet, H. J., Engelborghs, S., Wilssens, I., Paquier, P., & De Deyn, P. P. (2009). Cognitive, linguistic and affective disturbances following a right superior cerebellar artery infarction: A case study. *Cortex*, 45, 527–536.
- Marvel, C. L., & Desmond, J. E. (2010). Functional topography of the cerebellum in verbal working memory. *Neuropsychology Review*, 20, 271–279.
- Nichols, T. E., & Holmes, A. P. (2002). Nonparametric permutation tests for functional neuroimaging: A primer with examples. *Human Brain Mapping*, 15, 1–25.
- Noll, K. R., Sullaway, C., Ziu, M., Weinberg, J. S., & Wefel, J. S. (2015). Relationships between tumor grade and neurocognitive functioning in patients with glioma of the left temporal lobe prior to surgical resection. *Neuro-Oncology*, 17, 580–587.
- Nomura, E. M., Gratton, C., Visser, R. M., Kayser, A., Perez, F., & D'Esposito, M. (2010). Double dissociation of two cognitive control networks in patients with focal brain lesions. *Proceedings of the National Academy of Sciences of the United States of America*, 107, 12017–12022.
- O'Callaghan, C., Hornberger, M., Balsters, J. H., Halliday, G. M., Lewis, S. J., & Shine, J. M. (2016). Cerebellar atrophy in Parkinson's disease and its implication for network connectivity. *Brain*, 139, 845–855.
- Patay, Z., Parra, C., Hawk, H., George, A., Li, Y., Scoggins, M., ... Ogg, R. J. (2014). Quantitative longitudinal evaluation of diaschisis-related cerebellar perfusion and diffusion parameters in patients with supratentorial hemispheric high-grade gliomas after surgery. *Cerebellum*, 13, 580–587.
- Paternostro-Sluga, T., Grim-Stieger, M., Posch, M., Schuhfried, O., Vacariu, G., Mittermaier, C., ... Fialka-Moser, V. (2008). Reliability and validity of the Medical Research Council (MRC) scale and a modified scale for testing muscle strength in patients with radial palsy. *Journal of Rehabilitation Medicine*, 40, 665–671.
- Petersen, S. E., Fox, P. T., Posner, M. I., Mintun, M., & Raichle, M. E. (1988). Positron emission tomographic studies of the cortical anatomy of single-word processing. *Nature*, 331, 585–589.
- Pope, P. A., & Miall, R. C. (2012). Task-specific facilitation of cognition by cathodal transcranial direct current stimulation of the cerebellum. *Brain Stimulation*, 5, 84–94.
- Power, J. D., Barnes, K. A., Snyder, A. Z., Schlaggar, B. L., & Petersen, S. E. (2012). Spurious but systematic correlations in functional connectivity MRI networks arise from subject motion. *NeuroImage*, 59, 2142–2154.
- Qiu, T. M., Yan, C. G., Tang, W. J., Wu, J. S., Zhuang, D. X., Yao, C. J., ... Zhou, L. F. (2014). Localizing hand motor area using resting-state fMRI: Validated with direct cortical stimulation. *Acta Neurochirurgica*, 156, 2295–2302.
- Ramsey, L. E., Siegel, J. S., Baldassarre, A., Metcalf, N. V., Zinn, K., Shulman, G. L., & Corbetta, M. (2016). Normalization of network connectivity in Hemispatial neglect recovery. *Annals of Neurology*, 80, 127–141.
- Schmahmann, J. D. (2016). Cerebellum in Alzheimer's disease and frontotemporal dementia: Not a silent bystander. *Brain*, 139, 1314–1318.
- Schmahmann, J. D., & Sherman, J. C. (1998). The cerebellar cognitive affective syndrome. *Brain*, 121(Pt 4), 561–579.
- Shmuel, A., & Leopold, D. A. (2008). Neuronal correlates of spontaneous fluctuations in fMRI signals in monkey visual cortex: Implications for functional connectivity at rest. *Human Brain Mapping*, 29, 751–761.
- Siok, W. T., Niu, Z., Jin, Z., Perfetti, C. A., & Tan, L. H. (2008). A structural-functional basis for dyslexia in the cortex of Chinese readers. *Proceedings of the National Academy of Sciences of the United States of America*, 105, 5561–5566.
- Stoodley, C. J. (2012). The cerebellum and cognition: Evidence from functional imaging studies. *Cerebellum*, 11, 352–365.
- Stoodley, C. J., & Schmahmann, J. D. (2009). Functional topography in the human cerebellum: A meta-analysis of neuroimaging studies. *NeuroImage*, 44, 489–501.
- Stoodley, C. J., & Stein, J. F. (2011). The cerebellum and dyslexia. *Cortex*, 47, 101–116.
- Stoodley, C. J., Valera, E. M., & Schmahmann, J. D. (2012). Functional topography of the cerebellum for motor and cognitive tasks: An fMRI study. *NeuroImage*, 59, 1560–1570.
- Tan, L. H., Xu, M., Chang, C. Q., & Siok, W. T. (2013). China's language input system in the digital age affects children's reading development. *Proceedings of the National Academy of Sciences of the United States of America*, 110, 1119–1123.
- Taphoorn, M. J. B., & Klein, M. (2004). Cognitive deficits in adult patients with brain tumors. *Lancet Neurology*, 3, 159–168.
- Thiel, A., Habedank, B., Winhuisen, L., Herholz, K., Kessler, J., Haupt, W. F., & Heiss, W. D. (2005). Essential language function of the right hemisphere in brain tumor patients. *Annals of Neurology*, 57, 128–131.
- Thiel, A., Herholz, K., Koyuncu, A., Ghaemi, M., Kracht, L. W., Habedank, B., & Heiss, W. D. (2001). Plasticity of language networks in patients with brain tumors: A positron emission tomography activation study. *Annals of Neurology*, 50, 620–629.
- Tomasi, D., & Volkow, N. D. (2010). Functional connectivity density mapping. *Proceedings of the National Academy of Sciences of the United States of America*, 107, 9885–9890.
- Travis, K. E., Leitner, Y., Feldman, H. M., & Ben-Shachar, M. (2015). Cerebellar white matter pathways are associated with reading skills in children and adolescents. *Human Brain Mapping*, 36, 1536–1553.
- Tyler, L. K., Wright, P., Randall, B., Marslen-Wilson, W. D., & Stamatakis, E. A. (2010). Reorganization of syntactic processing following left-hemisphere brain damage: Does right-hemisphere activity preserve function? *Brain*, 133, 3396–3408.
- Van Dellen, E., Douw, L., Hillebrand, A., Ris-Hilgersom, I. H. M., Schoonheim, M. M., Baayen, J. C., ... Reijneveld, J. C. (2012). MEG network differences between low- and high-grade glioma related to epilepsy and cognition. *PLoS One*, 7, e50122.
- Van den Heuvel, M. P., Kahn, R. S., Goni, J., & Sporns, O. (2012). High-cost, high-capacity backbone for global brain communication. *Proceedings of the National Academy of Sciences of the United States of America*, 109, 11372–11377.
- Van Hees, S., McMahon, K., Angwin, A., de Zubicaray, G., Read, S., & Copland, D. A. (2014). A functional MRI study of the relationship between naming treatment outcomes and resting state functional connectivity in post-stroke aphasia. *Human Brain Mapping*, 35, 3919–3931.
- Verly, M., Verhoeven, J., Zink, I., Mantini, D., Peeters, R., Deprez, S., ... Snaert, S. (2014). Altered functional connectivity of the language network in ASD: Role of classical language areas and cerebellum. *NeuroImage Clinical*, 4, 374–382.
- Vogel, A. P., Maruff, P., & Morgan, A. T. (2010). Evaluation of communication assessment practices during the acute stages post stroke. *Journal of Evaluation in Clinical Practice*, 16, 1183–1188.
- Wang, Z. Q., Yan, C. G., Zhao, C., Qi, Z. G., Zhou, W. D., Lu, J., ... Li, K. C. (2011). Spatial patterns of intrinsic brain activity in mild cognitive impairment and Alzheimer's disease: A resting-state functional MRI study. *Human Brain Mapping*, 32, 1720–1740.
- Wen, P. Y., Macdonald, D. R., Reardon, D. A., Cloughesy, T. F., Sorensen, A. G., Galanis, E., ... Chang, S. M. (2010). Updated response assessment criteria for high-grade gliomas: Response assessment in neuro-oncology working group. *Journal of Clinical Oncology*, 28, 1963–1972.
- Winhuisen, L., Thiel, A., Schumacher, B., Kessler, J., Rudolf, J., Haupt, W. F., & Heiss, W. D. (2005). Role of the contralateral inferior frontal gyrus in recovery of language function in poststroke aphasia: A

- combined repetitive transcranial magnetic stimulation and positron emission tomography study. *Stroke*, 36, 1759–1763.
- Winkler, A. M., Ridgway, G. R., Webster, M. A., Smith, S. M., & Nichols, T. E. (2014). Permutation inference for the general linear model. *NeuroImage*, 92, 381–397.
- Wu, J., Lu, J., Zhang, H., Zhang, J., Yao, C., Zhuang, D., ... Zhou, L. (2015). Direct evidence from intraoperative electrocortical stimulation indicates shared and distinct speech production center between Chinese and English languages. *Human Brain Mapping*, 36, 4972–4985.
- Yan, C. G., Cheung, B., Kelly, C., Colcombe, S., Craddock, R. C., Di Martino, A., ... Milham, M. P. (2013a). A comprehensive assessment of regional variation in the impact of head micromovements on functional connectomics. *NeuroImage*, 76, 183–201.
- Yan, C. G., Craddock, R. C., Zuo, X. N., Zang, Y. F., & Milham, M. P. (2013b). Standardizing the intrinsic brain: Towards robust measurement of inter-individual variation in 1000 functional connectomes. *NeuroImage*, 80, 246–262.
- Yan, C. G., Wang, X. D., Zuo, X. N., & Zang, Y. F. (2016). DPABI: Data Processing & Analysis for (resting-state) brain imaging. *Neuroinformatics*, 14, 339–351.
- Yang, M., Li, J., Li, Y., Li, R., Pang, Y., Yao, D., ... Chen, H. (2016). Altered intrinsic regional activity and interregional functional connectivity in post-stroke aphasia. *Scientific Reports*, 6, 24803.
- Yang, Z., Wu, P. L., Weng, X. C., & Bandettini, P. A. (2014). Cerebellum engages in automation of verb-generation skill. *Journal of Integrative Neuroscience*, 13, 1–17.
- Zang, Y. F., He, Y., Zhu, C. Z., Cao, Q. J., Sui, M. Q., Liang, M., ... Wang, Y. F. (2007). Altered baseline brain activity in children with ADHD revealed by resting-state functional MRI. *Brain Development*, 29, 83–91.
- Zhang, H., Shi, Y., Yao, C., Tang, W., Yao, D., Zhang, C., ... Song, Z. (2016). Alteration of the intra- and cross- hemisphere posterior default mode network in frontal lobe glioma patients. *Scientific Reports*, 6, 26972.
- Zhang, Z. Q., Lu, G. M., Zhong, Y. A., Tan, Q. F., Chen, H. F., Liao, W., ... Liu, Y. J. (2010). fMRI study of mesial temporal lobe epilepsy using amplitude of low-frequency fluctuation analysis. *Human Brain Mapping*, 31, 1851–1861.

SUPPORTING INFORMATION

Additional supporting information may be found online in the Supporting Information section at the end of the article.

How to cite this article: Zhang N, Xia M, Qiu T, et al. Reorganization of cerebro-cerebellar circuit in patients with left hemispheric gliomas involving language network: A combined structural and resting-state functional MRI study. *Hum Brain Mapp*. 2018;39:4802–4819. <https://doi.org/10.1002/hbm.24324>